CATÓLICA
ESCOLA SUPERIOR DE BIOTECNOLOGIA
PORTO

SMART DATA-DRIVEN TOOL FOR PREDICTING AVOCADO FRUITS (*PERSEA AMERICANA*) SHELF-LIFE

by

Pedro Antunes E. L. Xavier

December 2022

CATÓLICA
ESCOLA SUPERIOR DE BIOTECNOLOGIA
PORTO

SMART DATA-DRIVEN TOOL FOR PREDICTING AVOCADO FRUITS (*PERSEA AMERICANA*) SHELF-LIFE

Thesis presented to *Escola Superior de Biotecnologia* of the *Universidade Católica Portuguesa* to fulfil the requirements of the MSc degree in Food Engineering

by

Pedro Antunes E. L. Xavier

Supervision: Professor Cristina L. M. Silva

Co-supervision: Professor Pedro Rodrigues

December 2022

To the loving memory of my grandfather Carlos.

Do not go gentle into that good night,
Old age should burn and rave at close of day
Rage, rage against the dying of the light.

Though wise men at their end know dark is right,
Because their words had forked no lightning they
Do not go gentle into that good night.

Good men, the last wave by, crying how bright
Their frail deeds might have danced in a green bay,
Rage, rage against the dying of the light.

Wild men who caught and sang the sun in flight,
And learn, too late, they grieved it on its way,
Do not go gentle into that good night.

Grave men, near death, who see with blinding sight
Blind eyes could blaze like meteors and be gay,
Rage, rage against the dying of the light.

And you, my father, there on the sad height,
Curse, bless, me now with your fierce tears, I pray.
Do not go gentle into that good night.
Rage, rage against the dying of the light.

Abstract

Recent years have seen a remarkable growth trend in avocado consumption, with projections that its exports will overpass those of pineapple by 2030, becoming the second most traded tropical fruit, just surpassed by the banana. When paired with their high unit value, this growth could make the avocado one of the most important fruit commodities of the next decades.

The economic relevance of avocado production has influenced its expansion into new regions of the world. Portugal is now the second largest producer of avocados in Europe, taking advantage of the climatic adequacy of the Algarve region to the requirements of this produce.

As the production of avocados is still limited to the tropical and subtropical regions, its exports are directly impacted by time-consuming distribution channels. Combined with the relatively high unpredictability of their post-harvest behaviour, this makes avocado fruits highly prone to wasteful practices.

The development of non-destructive tools that accurately trace the ripening process of avocado fruits could then be key to a better management of their shelf-life, optimizing their post-harvest handling to a point of drastically reducing distribution waste.

This project aimed to develop a smart data-driven tool that uses Machine Learning to improve the traceability of the ripening process of Hass avocado pears. A total of 476 avocados were divided between three storage groups, with different environmental conditions, and their ripening behaviour was traced by the implementation of an innovative 5-stage Ripening Index, that classified the ripening stage of each sample, daily, according to a set of common traits.

This information was paired with daily photographs of each avocado, to build a database of labelled image data that was then fed to two Convolutional Neural Networks, AlexNet and ResNet-18, taking advantage of the concept of transfer-learning where pre-trained knowledge is used to improve their adaptation to new sets of data.

The networks were trained to recognise the specific visual traits of each ripening stage, so that they could predict the state of new unlabelled data. This knowledge was tested on new datasets, reaching an average final accuracy of 77,8%, with an average of 88,4% of the predictions falling within a half-stage margin of error, and an average of 95,0% within one stage of the attributed classifications.

Both pre-trained networks achieved similar performances, with a slight advantage for ResNet-18, and the results were also similar across storage groups, suggesting that the predictive accuracy wasn't affected by the handling of the fruits.

These results represent an important step for the integration of Computer Vision tools on the post-harvest management of perishable products, which could not only improve shelf-life determinations, but ultimately be expanded into other assessments, with a major potential impact on waste prevention and quality improvement.

Keywords: Avocado; Smart Data; Ripening; Shelf-life; Data-driven prediction

Resumo

Os últimos anos têm registado uma clara tendência de crescimento no consumo de pera-abacate, com projeções a apontarem para que as suas exportações ultrapassem as do ananás até 2030, passando a ser o segundo fruto mais comercializado entre os de natureza tropical, apenas ultrapassado pela banana. Tendo em conta o seu elevado valor unitário, este crescimento poderia tornar o abacate numa das mais importantes mercadorias hortícolas das próximas décadas.

A relevância económica da produção de abacateiro influenciou a sua expansão para novas regiões do mundo. Portugal é agora o segundo maior produtor de pera-abacate na União Europeia, tirando partido da adequação climática da região do Algarve às especificidades desta cultura.

Dada a relativa limitação da cultura do abacateiro às regiões tropicais e subtropicais, as exportações de abacate são normalmente caracterizadas por longas redes de distribuição, o que quando combinado com o elevado grau de imprevisibilidade do seu comportamento pós-colheita, faz com que este seja um fruto altamente suscetível ao desperdício.

O desenvolvimento de ferramentas não-destrutivas que consigam acompanhar com precisão o processo de amadurecimento da pera-abacate podem ser o fator chave para uma melhor gestão do seu tempo de prateleira, otimizando as práticas de processamento e distribuição deste fruto, de forma a reduzir drasticamente a sua taxa de desperdício.

O objetivo deste projeto foi desenvolver uma ferramenta de gestão inteligente de informação, que usa Aprendizagem Automática para melhorar a gestão do amadurecimento de abacates Hass. Um total de 476 frutos foram divididos por três grupos de armazenamento, com diferentes condições atmosféricas, e o seu comportamento pós-colheita foi acompanhado através da implementação de um inovador Índice de Amadurecimento de cinco etapas, que classificou diariamente as amostras de acordo com um conjunto de características comuns.

A esta informação foram associadas fotografias diárias de cada abacate, para construir uma base de dados catalogada de imagens, que foram fornecidas a duas Redes Neuronais Convolucionais, AlexNet e ResNet-18, tirando proveito do conceito de Aprendizagem de Transferência, onde o conhecimento pré-adquirido pelas redes é usado para melhorar a sua adaptação a nova informação.

As redes foram treinadas para reconhecer as características visuais de cada etapa, de forma a conseguir prever o ponto de amadurecimento de frutos não classificados. Esta aprendizagem foi testada em novos conjuntos de imagens de pera-abacate, conseguindo-se uma precisão final média de 77,8%, onde uma média de 88,4% das previsões se encontraram dentro de uma margem de erro de meia etapa, e uma média de 95,0% com um máximo de uma etapa de diferença das classificações atribuídas.

Ambas as redes registaram performances semelhantes, com uma ligeira vantagem para a ResNet-18, e não se registaram diferenças significativas entre os três grupos, dando a entender que a precisão das previsões não terá sido afetada pelas suas condições de armazenamento.

Estes resultados representam um avanço importante para a integração de Visão Computacional na gestão pós-colheita de produtos hortícolas, que poderá não só trazer melhorias na determinação dos seus tempos de prateleira, como ser extensível a outras aplicações com potencial de grande impacto na gestão de qualidade e redução de desperdício.

Palavras-chave: Abacate; Aprendizagem Automática; Amadurecimento; Tempo de Prateleira

Acknowledgments

First and foremost, I feel like I owe a great share of my success to Professor Cristina Silva. She was a reference and became a friend, a source of inspiration, and someone I'll always look up to as one of the most important mentors of my life. Thank you for all the words of encouragement, and for the unrivalled dedication to science and education.

I was so excited when I realised that I would work with Professor Pedro Rodrigues, as I knew there was so much to learn from him. He was generous enough to listen through all the silly questions of an aspiring Food Engineer that knew very little about machine learning, always showing unconditional support and words of praise. I will forever be grateful for your mentoring, and I hope we meet again in the future.

To João Garcias and Global Avocados, thank you for supporting this project, proving that science and entrepreneurship can walk hand in hand in the pursuit of progress.

To everyone who worked in the *KitchenLab* with me, especially Marta Guimarães, part of this project is also yours. Thank you for your daily company, help, and motivation.

Mom and dad, here we are! Thank you for your guidance through every phase of my life, and for the unconditional love you've never failed to fill me up with.

To my sister Marta, who would say that cute little child would grow up to become my role model? I'm so proud of you and what you've accomplished. Thank you for lifting up my mood when no one else could. You're one of a kind.

To my grandfather Luís, making you proud is the greatest achievement I could ever aim for. Thank you for being a beacon of light in my darkest nights, for all the not-so-subtle jokes, and for your unmatchable generosity.

To my dear grandmother Maria Helena, I could never put in words how grateful I am to have grown up in the comfort of your lap. I'll always treasure the time we spend together. Thank you, from the bottom of my heart.

To my girlfriend Marta, whose name should be on the front page of this project, as I couldn't have done it without her. Thank you for telling me wrong whenever I doubted myself and for believing in me more than I ever did. Your generosity never fails to overwhelm me.

To Diogo and Joana, I hope you know how much I look up to the both of you. I'm honoured to have witnessed your growth, and to have shared with you more moments of pure joy than my memory can handle. Thank you for all these years of true friendship.

To Armando, probably the only person I can handle daily multi-hour-long conversations without never running out of topics. You've became family by affection, and I celebrate your success like my own. Here's to all those years when we kept the world in our pocket.

To all my professors, past and present, particularly one that I'll never forget: Ana Serôdio Fernandes. Years have made the seeds of your dedication sprout into my most treasured memories. The kind of ones that will last forever. Thank you.

To everyone that always believed in me. Thank you. This is just the beginning.

Contents

List of Figures

List of Tables

List of Abbreviations

AI – Artificial Intelligence

ANN – Artificial Neural Network

CNN – Convolutional Neural Network

CV – Computer Vision

DM – Dry matter

EU – European Union

ILSVRC – ImageNet Large Scale Visual Recognition Challenge

NIRS – Near-Infrared Spectroscopy

RH – Relative Humidity

T10 – Stored at a controlled temperature of 10 °C

T20 – Stored at a controlled temperature of 20 °C

Tamb – Stored at ambient temperature

UN – United Nations

UNECE – United Nations Economic Commission for Europe

1. Introduction

The determination and management of fruits and vegetables shelf-life is affected by multiple factors that are usually hard to track, as most of them experience changes that go beyond spoilage or contamination. Many of these products are sold in bulk and without any protective packaging, which make them even more susceptible to retail and consumers wasteful practices (Chakraverty & Singh, 2014).

The final quality of these perishable products not only depends on their pre- and post-harvest handling, but also on the intrinsic biochemical characteristics that directly affect their ripening process and the organoleptic changes that come with it (Chakraverty & Singh, 2014).

The traceability of these complex interactions between fruit and vegetables and their surrounding environment can be highly improved with the implementation of Artificial Intelligence (AI) systems, as they are particularly suited to intersect data from numerous sources and find relevant connections between them (Cheng et al., 2016; Lu & Lu, 2016).

There are indicators that the resulting data from these systems, commonly referred to as "smart-data", could be crucial to an integrated approach that will eventually lead to improvements in quality and waste prevention (Cheng et al., 2016; Lu & Lu, 2016).

1.1. Motivation

Avocado has been the fastest growing commodity among the major tropical fruits and is expected to remain so in the foreseeable years. Ample global demand and lucrative unit prices are the main drivers of this growth (OECD/FAO, 2021). As a climacteric fruit, its ripening process occurs during time-consuming distribution channels, with concerns over the unpredictability of its post-harvest behaviour causing a high degree of retail waste (Barman et al., 2015).

The application of Convolutional Neural Networks (CNN) is especially suited for the recognition of visual patterns with different levels of abstraction and has experienced a substantial growth in recent years (Aggarwal, 2018). Considering the significant visual changes that occur during the ripening process of 'Hass' avocado fruits, the most prominent being its pigment manifestations, that transit from a light green when unripe

to a purplish black when completely ripe, these could be the ideal subjects to study the potential accuracy of CNN-based predictions on their ripening stage.

While maintaining the understanding that visual data by itself would hardly be enough to accurately predict the shelf-life of a fruit, the intersection of these predictions with other relevant handling information could potentially be a breakthrough in the post-harvest management of avocados, eventually expanding its scope of application to other perishable products.

Literature research on the application of Machine Learning and Computer Vision[1] systems to the post-harvest management and quality control of fruits and vegetables suggests that this could be an underexplored subject. Considering the success of the implementation of these technologies in other fields, new and innovative exploratory works could have a breakthrough potential in the field of food engineering.

1.2. Scope

This project aimed to investigate how Computer Vision can be used to predict the ripening stage of avocado fruits (Persea Americana Mill.) of the Hass cultivar.

Data concerning storage conditions and texture analysis, such as the bioyield point and flesh firmness, was used to study and classify the progression of ripening factors along the shelf-life of multiple avocado fruits and paired with an image database in order to build and train predictive CNNs.

Finally, the capacity of the trained networks to accurately predict the ripening stage of new Hass avocado samples based solely on visual information was studied.

1.3. Innovation

The concept of Transfer Learning, which supports the idea that Machine Learning systems can easily be adapted to new sets of data using previously learned knowledge (Weiss et al., 2016), was explored in this research, both as a mean for smart computing resource management, but also to assess future extensions of its scope to other products.

[1] Computer vision is a field of computer science that aims to enable the automatized processing and identification of images and videos in the same way that human vision does.

Following this idea, the foundations of the project's designed networks were directly adapted from two well established CNNs, AlexNet and ResNet-18, whose architecture has been very successful in the field of image classification. Although these have not been initially thought for technical predictions of fruit and vegetable quality factors, their models can identify visual patterns in labelled datasets which can be useful when paired with new organized data.

The resulting data from multiple ripening assessments on the studied avocado fruits was combined into a 5-stage Ripening Index, which functioned as the classification labels that were paired with the daily collected images. The pairs of pictures and their respective ripening labels were fed to these networks using different methods to evaluate which would better serve the accuracy of the ripening predictions.

1.4. Graphical Abstract

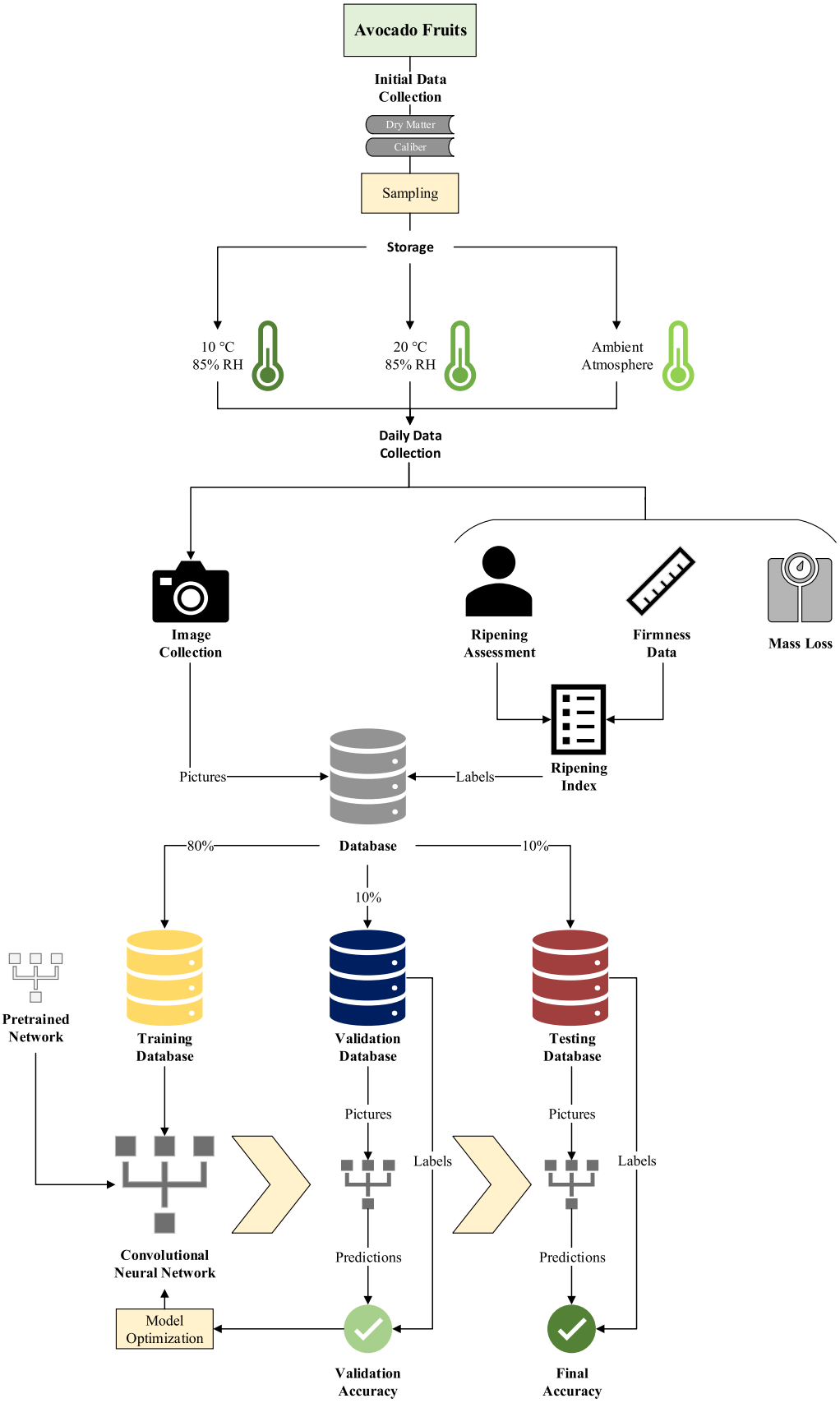

Figure 1 - Graphical Abstract.

2. State of the Art

2.1. Avocado Botany, Production, and Uses

The avocado pear is the fruit of the avocado tree (*Persea Americana* Mill.), which, at an economical level, is the most important member of the flowering plants family Lauraceae. This significance is rather recent, as for centuries throughout the human history its consumption was largely surpassed by another derivative of the Lauraceae family, the cinnamon, extracted from the bark of young twigs of the Ceylon cinnamon tree (Cinnamomum verum) (Rohwer, 1993), whereas the avocado fruit was mainly grown by small-scale farmers, mostly as part of indigenous agricultural systems, in and adjacent to its area of origin, in ancient Mesoamerica. It was only over the last 150 years that the avocado fruit experienced a dramatic market increase, to the point where it's considered today among the most important tropical and subtropical fruit crops in the world, having expanded into orchards and palates where it was previously unknown or rarely available (Bost et al., 2013).

Botanically, the avocado belongs to the genus Persea, which evolved in the ancient supercontinent of Gondwana, which is why its species are now scattered all around the world, though they thrived particularly in the landmasses that became North and South America, prospering in the warm and moist climates of the subtropical regions of these continents. Although avocados are now grown on every continent except Antarctica, its Mesoamerican heritage is undeniable, reason why its species became known as *Persea Americana* (Miller, 2020).

Like what happened with most other plants, the avocado went through intense crossbreeding and selection by humans, though its heterozygous nature that translates in a genetically related offspring, but with great phenotypic variations, makes the trees grown from seeds extremely unpredictable when it comes to the resulting fruit quality. Therefore, for orcharding purposes, avocado trees are almost universally propagated through grafting and budding, whereas seeds are mostly used by researchers to look for new desirable characteristics different from those expressed in the parent trees (Miller, 2020).

2.1.1. Cultivars

Nowadays, ‘Hass’ is, by a great distance, the most sought-after subtropical cultivar, with several new selections of ‘Hass’-like cultivars being the basis of the avocado fruit exports to Europe and the United States of America. Other commercially important subtropical cultivars include ‘Fuerte’, ‘Ettinger’ and ‘Pinkerton’, which were all selected from chance seedlings with superior fruit quality. To a lesser extent, some tropical cultivars are propagated through seedling (not grafted) trees, which results in horticulturally and nutritionally inferior quality fruits, mostly consumed locally in poor regions of the tropical lowlands. This is why though avocado can fall in the classification of both tropical and subtropical fruits, the subtropical cultivars take most of the worldwide market share (Cowan & Wolstenholme, 2016).

2.1.2. Global Trade Scenario and Future Projections

It is expected that, similarly to what has been happening in recent years, avocado continues to experience the fastest growth in output among tropical fruits, which is projected to reach 12 Mt by 2030 – more than triple of what was produced in 2010. With an ample market demand and a high value suited for exportation endeavours being the main drivers for this growth, it has seen substantial investments both in major and emerging production zones. Global exports of the avocado fruit are now of an equivalent quantity to the ones of mango and are expected to overcome the pineapple exports between 2025 and 2030, which would make it the second most traded fruit among the major tropical ones, only behind the banana. Given its aforementioned high average unit prices, this projection could place it as one of the most valuable fruit commodities (OECD/FAO, 2021).

The main importers of avocado fruit are the United States of America and the European Union (EU), where consumer interest has been fuelled by the fruit’s assumed health benefits. Both are expected to reach a joint 71% of global imports in 2030, although other countries like China and some Middle Eastern countries are also experiencing a rapid rise in imports. Mexico is expected to remain the world’s largest producer and exporter, with a global export share expected to reach 63% by 2030, despite the increasing competition from emerging exporters like Peru, Colombia, and Kenya, which account now for around 25% of the global exports (OECD/FAO, 2021).

Within Europe, France and Germany are the largest gross consumers of avocado, although Scandinavia has the highest *per capita* consumption. From 2016 to 2020, Portugal has experienced, by a great margin, the most growth in consumption among the European countries, with more than a 300% increase in this period, to an average of 0,96 kg *per capita* in 2020 (FRUITROP, 2021).

2.1.3. Production in Portugal

According to Eurostat, Portugal is the second largest avocado producer in the European Union, with a covered area of 2340 ha, and a yearly yield of 16.5 kt in 2020, numbers that are surpassed by Spain, which produced around 99.1 kt in the same period. Together, they account for over 90% of the total avocado fruits produced in the EU in 2020 (Eurostat, 2022). Most avocado crops grow in the southern regions of these countries, where the warmer climate accommodates the needs of this subtropical plant. At a national level, it's the Algarve region that stands out, with a cultivated area of avocado trees surpassing 1800 ha, which should correspond to around three-quarters of the total Portuguese production (Lopes, 2021).

Although the average productivity of this region is generally similar to one of the main avocado-producing countries, it has experienced some significant oscillations in recent years, attributed to occasional frosty weather which induces variations in flowering and fruiting. These variations seem to be correlated with intrinsic traits of the avocado tree, which make it more susceptible to adverse weather during key stages of fruit growth, and not particularly with the agricultural technological development or even the climate of producing countries, since some of the lower averages are seen in highly developed countries, and ones with similar climates usually present significant disparities in productivity (Duarte et al., 2020).

The cold sensitivity of this subtropical plant makes it particularly susceptible to frost damage, for which the introduction of the crop in the southern region of Portugal requires careful planning, that should consider the integration of anti-frost systems (Costa et al., 2018), as well as further research into the specific flowering and fruit setting aspects of the Atlantic, influenced Mediterranean climate, which presents different challenges from the ones where the avocado tree is native, where most of the current research takes focus (Duarte et al., 2018).

While the environmental impact of the introduction of new horticultural crops in the Iberian southern regions has to be thoroughly considered, including the impact on the soil and the local aquifers, as well as the carbon balance and the protection of the biodiversity, studies show that the exploration of avocado tree orchards can be an important asset for the community, with a relevant contribution to the local economy, and most importantly, reducing the dependence from the importation of those fruits from the far regions where they're traditionally produced (AGROGES, 2021).

Even though the high-level water consumption of this crop is not something to be ignored, it seems to be in line with the major crops produced in these regions, some of which have an even greater water consumption. Technology plays an important role in this scenario, and its smart application can practically eliminate all the resulting residues from the avocado orchards that are not particularly prone to plagues, fungi, or other diseases. Some Deep Learning systems are already being used by producers in Algarve for calibration and quality control (Freire, 2021; Lopes, 2021), but the integration of other monitoring systems in a digital framework, such as aerobotics to identify hydric stresses in the orchard blocks (Aerobotics, 2021), soil humidity probes to efficiently manage drip irrigation systems, and pH and electrical conductivity (for nutrient concentration) real-time control systems, might be the key for the sustainability of this high-value crop in the region (AZUD, 2021).

2.2. Avocado Maturity and Ripening

While its early growth follows the development pattern of most other fruits, experiencing rapid cell division leading to an increase in size, the avocado tends to continue growing while attached to the tree (Seymour & Tucker, 1993). However, unlike most other subtropical fruits, which normally reach their best eating quality when allowed to ripen on the tree or plant, avocados do not normally ripen until after harvest and can remain in a mature, but unripe condition until picked (Grierson, 2013; Kader, 2011).

The biochemical and physiological changes that fruits undergo during their maturation and ripening periods vary significantly depending on numerous factors, but it has been established that they can be generally divided into two main categories: climacteric and non-climacteric. The characteristics associated with the designation of climacteric fruits were originally attributed to a postharvest increase in the respiratory rate of many fleshy fruits, as is the case of the avocado, but the term is now rather associated with a burst of ethylene biosynthesis during the ripening process. Both of these processes play a defining role in the ripening phenomena, resulting in dramatic changes in colour, texture, flavour, and other organoleptic features of the fruit. Therefore, the understanding of these complex interactions is essential to the optimization of postharvest strategies, which can largely affect the quality and shelf-life of climacteric fruits (Grierson, 2013; Hiwasa-Tanase & Ezura, 2014).

2.2.1. Pre-harvest Maturity Assessment

Maturity at harvest is a determining factor in the storage life and final quality of the fruits, as it greatly affects their postharvest ripening, making them more susceptible to physiological disorders and mechanical damage (Kader, 2011). In the case of avocados, immature picked fruits may also fail to develop the appropriate flavour or texture when ripe (Seymour & Tucker, 1993). The fact that mature avocados do not show significant changes in colour and texture while in the tree, means that selecting the appropriate maturity level for harvesting must rely on quality assessments unrelated to those derived from visual external features (Ozdemir & Topuz, 2004).

There is a strong relationship between the maturation stage of the avocado fruit and a gradual decline of mesocarp moisture content, with a reciprocal increase in its relative dry matter. This is due to a steady increase in the oil content of the mesocarp during the

whole duration of fruit development, and a decrease in water by the same amount, whereas the percentage of water and oil contents put together always remains the same. Hence, oil and dry matter contents have been the most used parameters to define the standards of maturity among avocado cultivars, and although they can be assessed somehow interchangeably due to their strong correlation, the high cost of analysis and difficulty of measurements of the first made it generally be replaced by the latter in recent years (Magwaza & Tesfay, 2015).

Solvent extraction of the dehydrated mesocarp and refractive index techniques are the most commonly used methods for oil content determination in avocado fruits, while the dry matter and moisture content can be measured by drying flesh samples to a point where no further weight loss occurs. Although these can provide relatively accurate fruit maturity information, they rely on destructive and time-consuming methodologies, some of which can be only performed in laboratories (Magwaza & Tesfay, 2015). The emergence of automated technologies has enabled commercially feasible non-invasive methods for dry matter estimations, with near infra-red spectroscopy (NIRS) showing the most promising results in terms of cost-effectiveness, as opposed to the older and less commercially viable nuclear magnetic resonance (Wedding et al., 2013).

Recently there has been a growing adoption of portable NIRS devices that can non-invasively estimate, in a matter of seconds, the dry matter content of avocados and other fruits. Method and instrumentation optimization studies show promising results for some of these devices and their application on harvesting management, though they should require repeated measurements over time and along the multiple orchard blocks to be able to forecast target specifications with statistical relevance (Subedi & Walsh, 2020).

2.2.2. Ripening and Post-harvest Processing

The ripening process of the avocado fruit may start only a few days after harvest, as some inhibitory factors accumulated from the tree continue to show prevalence after the fruit has been abscised from the peduncle of the tree (Seymour & Tucker, 1993). This follows the idea that freshly picked tropical and subtropical fruits are organs that continue to experience a highly coordinated, genetically programmed, and irreversible developmental process (Osorio & Fernie, 2013), leading to the final stages of ripening characterized by senescence symptoms that eventually translate in the breakdown and

death of the fruit. Although none of these changes can be stopped, specific post-harvest treatments and techniques might delay or minimize their incidence and severity (Kader, 2011).

Lower storage temperatures have an inhibitory effect on the respiration rate and ethylene production rate, being one of the most obvious ways to delay the effects of ripening in climacteric fruits. It is important to notice though, that like most other tropical and subtropical fruits, avocados have a generally high chilling sensitivity, which can lead to internal injuries. Although this varies among different cultivars (Seymour & Tucker, 1993), studies indicate that for the Hass variety, the best final quality was obtained with fruit cool stored at 4 – 6°C, and later ripened at 15°C. Higher ripening temperatures, especially above 30°C, showed significantly higher levels of rots and vascular browning, while temperatures below 4 °C resulted in uneven ripening and chilling injuries. As postharvest rots usually derive from latent infections initiated in the tree during the growing season, longer storage periods also tend to result in more evident signs of poor quality (Hopkirk et al., 1994). According to Woolf et al. (2020), some exporters use a step-down temperature regime for long-distance shipping, where the storage temperature is set to slowly decrease to allow the fruit to acclimate to lower temperatures without inducing chilling injury (Woolf et al., 2020).

While other plant hormones interfere with the ripening process of the avocado fruit, such as auxins (Davies & Böttcher, 2014), ethylene is the one that has received the most attention. The study and interpretation of the genetic signalling components of these hormonal networks can provide further insight into how we could make use of genomic resources for crop improvement, potentially leading to the manipulation of the ripening process (Kumar & Sharma, 2014).

The management of ethylene exposure in storage can also have beneficial effects on the ripening strategies for avocado fruits, preventing the undesired accelerated softening and deterioration that might happen during transportation and storage, as the presence of ethylene in cold storage facilities, either in the air or in a controlled atmosphere can significantly reduce the storage life of these fruits, for which the severity of the damage will depend the its concentration, duration of exposure and storage temperature. Adequate air ventilation or even the use of ethylene scrubbing technologies such as potassium permanganate will minimize this decay while holding the facilities at the lowest safe temperature will also delay its effects (Kader, 2011). Sources of ethylene should also be

avoided in and around avocado storage facilities, such as other climacteric fruits, combustion engines, fire, and cigarette smoke (Woolf et al., 2020).

The pigment changes that occur during the ripening of the avocado fruits, which usually go from green to purple/black during this time, are an important ripeness indicator for handlers and consumers. These changes are only partly related to the chlorophyl concentration on the skin of the fruit, which undergoes a slight decay after harvest, remaining relatively unchanged for the rest of the ripening period, but rather with external factors which result in increased biosynthesis of anthocyanins, specifically the cyanidin 3-*O*-glucoside. Growing environment and ripening temperatures are highly correlated with the increase in the synthesis of these pigments, for which avocados ripened at higher temperatures may develop earlier and stronger purple/black pigmentation, while the ones ripened at lower temperatures can even become soft while showing little skin darkening (Cox et al., 2004).

This represents a great challenge to the classification of avocado fruits according to their ripening stage, as though colour and texture changes can provide important information about this process, they must be complemented with non-visual data according to their postharvest handling. The application of image processing and Computer Vision (CV) systems could provide a cost-effective, non-invasive, high-accuracy methodology for ripening index classification, but it would require large amounts of samples, from different sources and storage conditions, to be able to create predictive models of these complex interactions (Arzate-Vázquez et al., 2011).

The large heterogeneity of the avocado fruit's ripening process, which is still not fully understood, is probably the biggest drawback in the implementation of ripening index estimation technology, suggesting that integrated approaches that can trace and correlate all pre and postharvest factors that might influence the ripening behaviour of the fruit, making use of innovative methods for non-destructive on-chain analysis, are possibly the best solution to achieve better consistency among quality parameters, potentially minimizing its retailing and household waste (Hernández et al., 2016).

2.3. Applications of Smart-Data in the Agro-Food Industry

The impact of the COVID-19 pandemic brought a setback in the efforts to end food insecurity, with the United Nations (UN) goal of achieving Zero Hunger by the year 2030 seeming to be an increasingly challenging perspective. A worldwide integrated approach, that finds sustainable and inclusive ways of increasing productivity while significantly reducing food loss and waste, is seen as the only scenario that tackles the persistent disparities shown across different regions of the globe, with women and children being the most vulnerable (FAO et al., 2022). These measures will only be effective if they take into consideration the socioeconomic reality of the most affected groups, reducing the cost and affordability of a healthy diet throughout the entire population, by reallocating food and agricultural policies in favour of ones which successfully broaden the global access to nutritious and better-quality food, such as the generation and transferring of knowledge and innovation, the protection of biodiversity and natural resources and fair global trading (FAO et al., 2021).

This kind of multistakeholder holistic approach is already being discussed within the scope of many UN Sustainable Development Goals (SDGs), where a transition from a linear to a circular economy model is seen as the key to addressing the root causes of the most pressing sustainable development challenges, empowering communities and providing them with the appropriate tools to create local-based solutions that still make sense in a global scenario (Sutherland & Kouloumpi, 2022).

According to a report by Ellen MacArthur Foundation (2019b), for every dollar spent on food, society pays two dollars in health, environmental, and economic costs, half of which – totalling USD 5.7 trillion each year globally – are due to the way food is produced. These are a direct result of the 'linear' nature of modern food production, which extracts finite resources, is wasteful and polluting, and harms natural systems (Ellen MacArthur Foundation, 2019b).

The complex shift from an economy that sustains its growth in the depleting of resources, to one that designs out waste by keeping products and materials in use, repurposing them along the cycle, will be greatly accelerated if we take advantage of new technologies, that will integrate faster learning processes, iterative cycles of designing, and which can easily gather feedback and improve upon themselves. Artificial Intelligence systems can be the defining elements of this systemic transition, as they

would complement and expand upon people's skills and help to make better sense of the abundance of data that will need to be taken into consideration (Agrawal et al., 2021; Ellen MacArthur Foundation, 2019a).

The application of Computer Vision and Machine Learning technologies in the agricultural scenario, commonly referred to as smart farming and considered a key element to develop sustainable practices (Walter et al., 2017), is already an ongoing reality for crop yield predictions, soil properties analysis and irrigation management. Many different ML algorithms are also being used to simulate effective models for weather prediction and crop quality management, providing stakeholders and farmers with precision tools that support ideal decisions. Researchers are now using Deep Learning models to predict fruit ripening stages and fruit maturity, which might be extremely useful in defining harvesting times and post-harvest storage conditions that will potentially improve quality and extend the shelf-life of produce (Sood & Singh, 2021).

Literature research shows that in recent years, studies of the application of Machine Learning for shelf-life predictions have been explored in relation to fruits and vegetables (Ceelen, 2019), but the integration of visual data through Computer Vision Systems in order to develop predictive models that work mainly from image processing appears to be underexplored in relation to other fields of engineering (Sood & Singh, 2021). The potential development of such models could have the advantage of being very cost-effective since the data needed to feed them can be easily obtained with any handheld camera (Bhuyan, 2020).

Reports indicate fruits and vegetables as the type of foodstuff that's more prone to wasteful practices (United Nations Environment Programme, 2021). Innovative systems are being considered to monitor, in real-time and along the whole supply chain, multiple quality features that affect the shelf-life of perishable products. Variations in storage conditions along the distribution chain may be responsible for major losses which could potentially be avoided with integrated management of food quality data. These predictive models are yet still dependent on human sensory assessments of quality features, functioning mostly as a complement to help identify the source of potential problems (Torres-Sanchez et al., 2020). It's therefore important to find ways to extend the usage of AI technologies and take greater advantage of its emerging opportunities, which can lead to major developments in the whole food industry (Kumar et al., 2021).

The implementation of holistic AI systems that minimize food loss will only get us so far. It's important to also make use of these systems, paired with the emerging interfaces of the Internet of Things, to achieve significant changes on the consumer stage (Ramadoss et al., 2018), where most of this waste happens. Also, diverging from earlier narratives, household food waste per capita seems to be broadly similar across different income groups, suggesting that action on food waste is equally relevant in the high, upper-middle, and lower-middle-income countries. This emphasizes the importance of developing and implementing new ways of understanding how and why this waste happens, which might differ greatly within different socio-economical standards, for example by the use of smart-bin technology, or other systems that scan food as it becomes waste (United Nations Environment Programme, 2021).

Although improvements in integrating data along the supply chain are very much essential for a less wasteful reality, the cycle won't be closed until ways are found of extending the scope of approach to a repurposing stage, where AI can contribute to the valorisation of food by-products by helping to design out potential contaminants from organic material streams, creating products that can easily re-enter the chain or safely return to soils as organic fertilizers. AI-assisted product development is already being used by companies to design plant-based meat alternatives, and in the future that can be extended to help source regeneratively grown ingredients, reduce processing waste, and avoid unsafe additives, promoting the overall access to healthy food (Ellen MacArthur Foundation, 2019a).

It is also important to notice that this transition will not likely happen all at once, which makes it so that these so-called 'circular' products will have to be competitive in the marketplace and present themselves as a better overall choice for all stakeholders. One way to do that is by establishing dynamic prices across the whole cycle, which make use of reverse logistics that forecast the fluctuations of the supply and demand dynamics, crossing that information with shelf-life data to apply fair prices that balance out the precepted value of the products' quality features. For perishable products, this would imply the implementation of automated ways of accurately tracing shelf-life predictions (Cruz et al., 2019; Scholz & Kulko, 2022).

Considering that visual inspection and image analysis are the primary types of assessment for most quality factors of food products, with a direct impact on market-price and shelf-life determinations, it seems straightforward that the development of CV tools

will translate into a growing adoption of these technologies for quality assurance tasks, most of which are highly repetitive and can be somewhat subjective, leading to more consistent and cost-effective decisions than those taken exclusively by human approach (Blasco, 2012).

The revolutionary architecture of Convolutional Neural Networks (CNNs) has brought the applications of CV systems in the food industry much beyond image processing and pattern recognition (Kakani et al., 2020; Nayak et al., 2020). Published literature has compiled many of the current and potential applications for CV technology in food quality evaluation, referring to promising works that would allow for automated detection of surface and internal defects in apples, and even multispectral scattering imaging that could potentially evaluate their firmness. These non-destructive methods of quality evaluation, specifically the ones that tackle properties that typically don't show up at the surface of fruits, could achieve ground-breaking improvements in consumer acceptance and confidence in fruits and vegetables (Lu & Lu, 2016). Also, works on the automated grading of strawberries, that take into consideration size, shape, and ripeness (the latter being the most challenging to define given its complexity), have shown promising results that could successfully be applied in online post-harvest systems, with significant improvements on quality and safety management (Cheng et al., 2016).

To make better use of these tools, non-destructive methods for quality data collection also need to improve. Packhouses constitute the intermediate stage between farm production and retail sellers, and it is where most of the mechanical handling takes place. For fruits like avocados, which are regularly subject to long transportation chains given their subtropical nature, this stage can largely affect the quality features of the fruit, to a point that is currently not yet fully understood. The lack of non-destructive instrumentation at this stage makes it a challenge for ML models to accurately predict its implications. Researchers have now developed smart synthetic sensors, with a structure that morphologically simulates that of the fruit they monitor, which can record both environmental and physical stresses experienced by the fruits during the post-harvest handling period. The idea is that these sensors are treated by handlers the same way they treat the fruits, package alongside them and going through the same processing units (Broekman & Steyn, 2021; Broekman et al., 2020).

As data collection constitutes a defining factor for the scalability of ML models, this and other types of data gatherers are crucial not only to achieve full traceability of the

products but also to provide additional sources of data to improve the accuracy of other AI systems like the ones which evaluate quality. It will be equally important to improve data management systems to ones suited to handle a huge amount of data with the needed speed, flexibility, and reliability. Given the heterogeneity of data sources, reliable big data transferring software will also need to be implemented, that can move data from sources like consumers' mobile phones or retailers' databases into nonrelational, open source and horizontally scalable data clusters referred to as NoSQL (Marvin et al., 2017).

Despite all these advantages, it is important to also consider the limitations and drawbacks of a full AI-assisted circular transition. Like it happened with other revolutionary transitions in history, these technologies can create unexpected stresses in the employment standards of society, with those with lower income being usually the most affected. The high maintenance of these systems, which will need to be constantly monitored and updated, will also add a huge cost to their operability, which in the worst case could even cause in an increase in prices if managed incorrectly. An AI-assisted circular economy should add environmental and social protection to the value chain, but its social implications, high energy consumption, e-waste production, market concentration, and the whole ethical framework will have to be considered, or else it could end up defeating its purpose (Agrawal et al., 2021).

2.4. Deep Learning and Artificial Neural Networks

Artificial Neural Networks (ANNs) are the base of machine learning environments and take inspiration from the neurological systems of biological organisms. The goal is to process inputs that are attributed to individual neurons, which are then scaled with weights that affect the function computed at each unit. The propagation of those weights as intermediate parameters originates a path from the input neurons to the output neurons (Graupe, 2013).

Just as external stimuli are used by biological organisms to learn and adapt, in the case of ANNs, those stimuli are provided by the training data, containing examples of input and output pairs of the function to be learned. An example of this in practice is a training dataset comprised of images (inputs) and their annotated labels (e.g., carrot, banana) as the desired outputs. These training data pairs are fed into the neural network by using input representations to make predictions about the output labels. The training data should then provide feedback on the correctness of the weights used between those pairs, which are then adapted throughout the training process to provide for accurate predictions and should result in an increasing matching accuracy between the images and the annotated output labels in the training data. The goal is to then apply these trained networks to other inputs, that have not yet been labelled, and get accurate predictions for those outputs, which would allow scaling the training knowledge to much bigger datasets (Aggarwal, 2018).

2.4.1. Image Classification and Convolutional Neural Networks

The relevance of spatial dependency in the grid-structured data that forms a 2-dimensional image requires an approach that considers the relative location of each element in the matrix. Convolutional Neural Networks (CNNs) are a type of ANN designed to work with grid-structured inputs which have strong spatial dependencies in local regions of the grid, for which they are by far the most used architecture to process image data in machine learning, although one can also use these networks for all types of temporal, spatial and spatiotemporal data (Aggarwal, 2018).

An example of this spatial dependency can be observed when shifting an element across the grid structure, which should maintain the same interpretation. This level of translation invariance, an important property of image data, is why when looking at, for example, a banana, the output should be independent of whether the fruit was on top or the bottom

of an image. CNNs tend to create similar feature values from local regions with similar patterns, which makes them ideal to analyse this kind of data (Aggarwal, 2018).

CNNs are considered one of the greatest success stories of biologically inspired artificial intelligence, as their key design principles were mostly drawn from neuroscience. Neurophysiologists David Hubel and Torsten Wiesel have been acknowledged with the Nobel Prize in Physiology or Medicine in 1981 (NobelPrize.org, 2022) for their exploratory works on mammalian vision systems, in which the study of the cat's visual cortex provided early motivation for the CNN architecture. Among many aspects of brain function, they discovered that the cat's visual cortex has small regions of cells that are sensitive to specific regions in the visual field, which make them great at identifying the shape and orientation of different elements. These cells are then connected using a layered architecture, which suggested that mammals use these different layers to construct portions of images at different levels of abstraction (Aggarwal, 2018; Goodfellow et al., 2016).

The extrapolation of these findings into an artificial system was the breakthrough point of the CNN architecture, which achieves something similar by encoding primitive shapes in earlier layers, and more complex shapes in later layers. One of the first applications of such models was in the recognition of handwritten numbers in checks, in the early 1990s, which led to more and more complex systems, as computation power improved, eventually opening the way to real-time object detection in images, facial recognition, gesture reading and many other innovations that are now implemented into many technological systems (LeCun et al., 2010).

One of the most relevant trackers of this technological progression has been the annual ImageNet competition (Stanford Vision Lab, 2020), which took place between 2010 and 2017 and challenged researchers into perfecting deep network architectures that improve upon the established ones to resolve harder tasks in computer vision. **Table 1** summarises some of the most promising contesting networks of this challenge, and how fast they improved in accuracy over a short span of time.

The fact that practically all competitors used some form of CNN is taken as proof of its fitness for image classification. One of the earliest methods to stand out in this competition was AlexNet, which was trained to classify the 1,2 million high-resolution images in the ImageNet LSVRS-2010 contest into the 1000 different classes, with an innovative architecture that significantly improved training times, for example by using

multiple GPUs, and reduced the probability of overfitting through data augmentation and dropout methods (Krizhevsky et al., 2017).

The success of this model opened a path that tackled one of the greater challenges faced by image data analysts, which not always had access to enough labelled training data to train a network for a particular application. Taking advantage of the fact that extracted features from a particular source of image data can be highly reusable across different sources, the emergence of pretrained networks allowed to make use of those sets of features, which could, later on, be adapted to different, more limited datasets, by extracting multidimensional features from the fully connected layers. This type of off-the-shelf feature extraction approach (Razavian et al., 2014), depicted as a type of transfer learning, became so common over the years, that analysts rarely train CNNs from scratch anymore. It makes use of a prominent feature in CNNs in which the weights of the early layers can be generally transposed between data pools without loss of relevance, reserving most of the computing power to train only deeper layers, which will then fine-tune to the more complex features particular of each training set (Aggarwal, 2018).

After the great success of AlexNet, other pre-trained models improved upon its accuracy, not only by implementing new ways of taking the most out of the limited computing power available but also by evolving into more complex architectures, with more hidden layers in between the input and output that allowed them to recognize increasingly specific features of image data. A recent example of this network is ResNet, which won the 2015 ILSVRC competition and uses 152 layers (in comparison with the eight layers of AlexNet). It achieved a top-5 error of 3.6%, which resulted in the first classifier with human-level performance (He et al., 2016).

The success of this architecture was largely due to the innovative way it approaches a common challenge of deeper neural networks, which become very difficult to train as they grow more complex, as the standard hierarchical model implies that all concepts in the image grow to the same level of abstraction as they move forward in the network path (Aggarwal, 2018; He et al., 2016). Aggarwal (2018) gives a good example of this: “Consider a circus elephant standing on a square frame. Some of the intricate features of the elephant might require a large number of layers to engineer, whereas the features of the square frame might require very few layers. Convergence will be unnecessarily slow when one is using a very deep network with a fixed depth across all paths to learn concepts, many of which can also be learned using shallow architectures. Why not let the

neural network decide how many layers to use to learn each feature?". This change from a hierarchical model to an iterative one, reformulating the layers as learning residual functions concerning the layer inputs, instead of learning unreferenced functions, allowed ResNet to make greater use of the major increase in depth of its architecture, without becoming redundant to the point of loss of value (He et al., 2016; Veit et al., 2016).

Table 1 - The number of layers in various top-performing ILSVRC contest entries. Source: (Aggarwal, 2018)

Name	**Year**	**Number of Layers**	**Top-5 Error**
-	Before 2012	≤ 5	> 25%
AlexNet	2012	8	15,4%
ZfNet	2013	8 / > 8	14,8% / 11,1%
VGG	2014	19	7,3%
GoogLeNet	2014	22	6,7%
ResNet	2015	152[2]	3,6%

2.4.2. Transfer Learning and Deep Network Design

The application of transfer learning models to the aforementioned pre-trained networks, allows them to serve as foundations for the development of a much wider range of applications, not only because they significantly reduce the computing power required to train a new network, but also for their contribution to decreasing the minimal quantity of data needed to feed the training dataset (Weiss et al., 2016). This concept, which was already discussed about machine learning and data mining algorithms before the rise of CNN architectures, is highly motivated by the fact that people can intelligently apply previously assimilated knowledge to solve new problems in a faster and more educated way. That is, someone that is already proficient in playing the guitar will generally be

[2] The results of the ResNet in the ILSVRC contest were obtained from an ensemble boosting of six different models, with the following number of layers: 34A, 34B, 34C, 50, 101, and 152

able to learn how to play the piano much faster than someone with no musical background. In the same way, if we train a network to recognize apples, it will then be much easier to train it to recognize pears (Pan & Yang, 2010).

One of the platforms that makes use of this concept is the multi-paradigm numeric computing environment MATLAB, which makes use of a proprietary programming language developed by MathWorks (Voloşencu, 2022), which included, since their R2018b instalment, a Deep Learning Toolbox, providing a framework for designing and implementing deep neural networks (MathWorks, 2022a; Paluszek & Thomas, 2020), that can also load pretrained networks, view and edit their layer properties, adding new layers and connections to make the best use of transfer learning, with an architecture that can easily be adapted to a new set of training data (MathWorks, 2022b).

3. Objectives

The objectives of this research are:

1. Build a photographic database that tracks the ripening process of a set of avocado fruits.
2. Study the correlation between the intrinsic characteristics of the ripening process of avocados and their visual manifestation.
3. Evaluate the effect of storage temperature on the ripening process of avocados.
4. Develop Deep Learning Networks that can predict the ripening stage of each avocado, based solely on visual inputs.
5. Study the performance of the developed networks and possible integration with other non-destructive ripeness assessment methods.

4. Material and Methods

4.1. Initial Procedures

4.1.1. Sampling

A total of 478 avocados (*Persea Americana* Mill. cv Hass) were obtained directly from a supplier based in Tavira, Portugal. All of them were sourced from a group of local producers and harvested on the same day in March 2022. The fruits were transported in a refrigerated truck at 5 °C and delivered to the CBQF research centre in Porto, Portugal within the third day of post-harvest.

Upon reception, the avocados were thoroughly washed and scrubbed using a solution of sodium hypochlorite with $0{,}16g$ of active chlorine per liter. All fruits were then labelled, weighted, and sorted between ten boxes so that each box had 47 samples of evenly distributed weights. The remaining eight samples were used for the initial dry matter calculations.

4.1.2. Storage

The boxes were then distributed in three categories, according to the temperature and relative humidity (RH) of storage. Two of these were submitted to a controlled environment, with stable temperature and RH profiles, and a third one was left at room conditions, to evaluate how floats in the storage profile would affect the visual accuracy of the predictions. The three groups are detailed as follows:

- **T10** – 4 boxes (188 samples) stored at a controlled temperature of 10 °C and 85% RH;
- **T20** – 3 boxes (141 samples) stored at a controlled temperature of 20 °C and 85% RH;
- **Tamb** – 3 boxes (141 samples) stored at ambient temperature, with variable RH.

For the controlled temperature storage, the boxes were stored in climactic chambers, a *Fitoclima 1200 (Aralab)* for the T10 group and a *Fitoclima 600 (Aralab)* for the T20 group.

The boxes belonging to the Tamb group were left in the *Laboratory of Food Processing Engineering*, exposed to the ambient air and light.

For all groups, variations in temperature and humidity were tracked throughout the whole experiment using IBS-TH1 (*Inkbird*) Bluetooth temperature and humidity probes.

4.1.3. Initial Dry Matter Calculations

Upon receiving the avocado fruits, eight samples were randomly selected for the initial dry matter assessments. These were made according to the official method of analysis for fruit samples, published by AOAC International (AOAC, 2000)

After opening the fruits, three small samples of their flesh were extracted from each. These were placed in previously weighted Petri dishes and then weighted again to assess the total mass of each flesh sample. All samples were labelled, and their raw flesh masses were registered.

The petri dishes containing the flesh samples were placed in a dehydrating oven and left exposed to a 103°C circulating hot air for 24 hours. The samples were then weighted again, the weight of the empty petri dish subtracted to find the dehydrated flesh mass, and their dry matter assessed using the following calculations:

$$DM\ (\%) = \frac{raw\ flesh\ mass\ (g)}{dehidrated\ flesh\ mass\ (g)} \times 100\% \quad (1)$$

The dry matter contents from the flesh samples belonging to the same fruit were averaged to obtain weighted values, and the results from the eight studied fruits were compared with the typical values practiced in the food industry for the determination of the appropriate harvesting maturity stage.

4.2. Image Collection

From the fifth post-harvest day onward, two photographs were taken daily from each sample, on opposite sides of the fruit, to maximize the covered area. These were paired with information about each sample's **Ripening Index**, explained ahead, to build a categorized database.

4.2.1. Equipment

The samples were photographed in a HAVOX-HPB-40D Photo Studio Lightbox (42 x 42 x 42 cm), with a matt white backdrop, illuminated by two LED ramps with a luminous flux of 12000 lm ± 200 lm and a colour temperature of 5500 K, paired with a light diffuser cloth.

The photos were obtained using a Canon EOS 60D DSLR camera, with the Canon EF-S 18-55mm f/3.5-5.6 IS II lens, mounted on the top of the studio box.

4.2.2. Procedure

Each box containing the avocado fruit samples was collected from its respective storage, one at a time, and placed in the Kitchen Lab, where the photographs were taken.

Each sample was then placed inside the studio lightbox, using a small flexible mount, moulded individually to secure it in place. To allow for consistency throughout the whole duration of the experiment, the samples were all firstly aligned by centring their stem directly perpendicular to the camera, the camera focus point was checked and adjusted, and the first shot was taken. The samples were then rotated 180 degrees to take the backshot.

The following camera settings were used:

ISO: 100; Aperture: 8.0; Shutter Speed: 1/20 s

The photographs were collected using the EOS Utility 2 Software (*Canon Inc.*), and labelled according to the sample number, front or back position, storage temperature, and date of collection.

A database was built attaching this information to the image files and was later on updated to include the Ripening Index classification of each sample, described in the following chapter.

4.3. Ripening Index

To train a Convolutional Neural Network to make predictions on the ripening stage of avocado fruits, a set of classification labels must be assigned to the provided data. Although the ripening process has a continuous nature, a sequential index can provide a better categorization of the image sets, which will therefore allow the network to learn how to differentiate their respective traits and make predictions on new sets of data.

A Ripening Index was adopted that classified each sample between 1-5, corresponding to the following stages of the ripening process:

1. Unripe
2. Breaking
3. Ripe (First Phase)
4. Ripe (Second Phase)
5. Overripe

These were assessed by a team of two trained researchers and were based on a set of common visual and texture traits for each stage, which are detailed ahead.

4.3.1. Stage 1 – Unripe

The first stage of the Ripening Index is characterized by a yellowish hue green colour, and a very firm texture. The fruits might show signs of sun damage or other marks associated with its pre-harvest conditions. The following figure (**Figure 2**) is an example of a Hass avocado fruit at this stage:

Figure 2 - Example of a Stage 1 (Unripe) sample.

4.3.2. Stage 2 – Breaking

In the second stage of the Ripening Index, signs of ripening start to manifest in a darkening pigmentation, which should now be of a greyish olive green with hues of brown. It remains with a firm texture, though it should give slightly when pressed (**Figure 3**).

Figure 3 - Example of a Stage 2 (Breaking) sample.

4.3.3. Stage 3 – Ripe (First Phase)

As the avocado fruit becomes ripe, shades of purple start to appear, scattered along the skin. Its texture is now less firm to the touch, signs of an easily sliced flesh, which should yet resist to mashing (**Figure 4**).

Figure 4 - Example of a Stage 3 (Ripe – First Phase) sample

4.3.4. Stage 4 – Ripe (Second Phase)

The fourth stage of the Ripening Index is considered the last one of its shelf-life, where its ripeness is at the maximum value but with no relevant signs of senescence or degrading quality. Its skin should now be of a homogenous purple shade, and its flesh easily displaced by the slight touch. The stem should appear dry and of a light brown colour (**Figure 5**).

Figure 5 - Example of a Stage 4 (Ripe – Second Phase) sample

4.3.5. Stage 5 – Overripe

In the fifth and last stage of the Ripening Index, the fruit shows clear signs of senescence, with the appearance of mould spots throughout the skin and around the stem. In terms of texture, a separation between the exocarp and the mesocarp can be observed (**Figure 5**).

Figure 6 - Example of a Stage 5 (Overripe) sample.

4.4. Firmness Assessment

For the whole duration of the study, three samples from each storage group were randomly selected every second day and subjected to firmness assessments using a texture analyser. This was performed using a *TA.XTplus* machine, connected to a computer using *Exponent Connect* software by Stable Micro Systems©.

For every sample, six perforations were made by a cylindric probe with a diameter of 3mm, to a total length of 15mm over ten seconds. This should be enough to pierce the skin and go through the flesh of the fruit without getting too close to its seed, which could affect the flesh firmness results.

The textural data was analysed by the software, to return information about the bioyield point of the avocado fruits and to assess the firmness of their flesh.

Figure 8 shows an example of the data plot from an avocado perforation test. An automatized set of instructions was designed to look for the point of maximum force of each test run and classify it as the bioyield point. This should correspond to the moment where the skin is punctured, which results in a sudden fall of the displacement force, as the flesh underneath it is of a softer nature. Next, the system would take the average force from that point, up until the end of the perforation, which was taken as the flesh firmness (Bourne, 2002).

The resulting data was compared with the Ripening Index classifications, to study the differences between the visual assessment of the avocado fruits' ripeness and the firmness of their skin and flesh.

Figure 7 - TA.XTplus

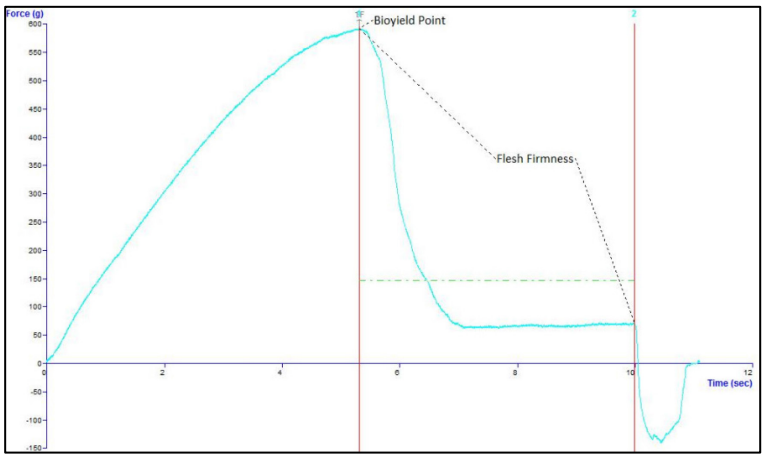

Figure 8 - Example of a data plot from an avocado perforation test.

4.5. Convolutional Neural Network (CNN) Design and Architecture

The application "Deep Networks Design", included in the software MATLAB R2021a from MathWorks Inc., was used to build two CNNs, based on two publicly available pre-trained networks: AlexNet and ResNet-18.

4.5.1. Training Procedures

Each network was trained on eight different datasets. Two non-discriminative, one where the classification labels were the 1-5 scale Ripening Index, and one where these were converted to a 1-9 scale Ripening Index, to allow for a future application of a margin of error. Six discriminative datasets were used to train each network, three for each Ripening Index model, where the database was split according to storage conditions, to verify whether the accuracy of the network was affected by the different handling groups.

The following scheme (**Figure 9**) describes the sixteen trained networks, eight for each pre-trained network (AlexNet and ResNet-18), where the non-discriminative data pools were used to study the general accuracy of the networks with both classification types (5-stage and 9-stage), and the discriminative data pools provided feedback on whether the different storage conditions would affect the accuracy of the predictions.

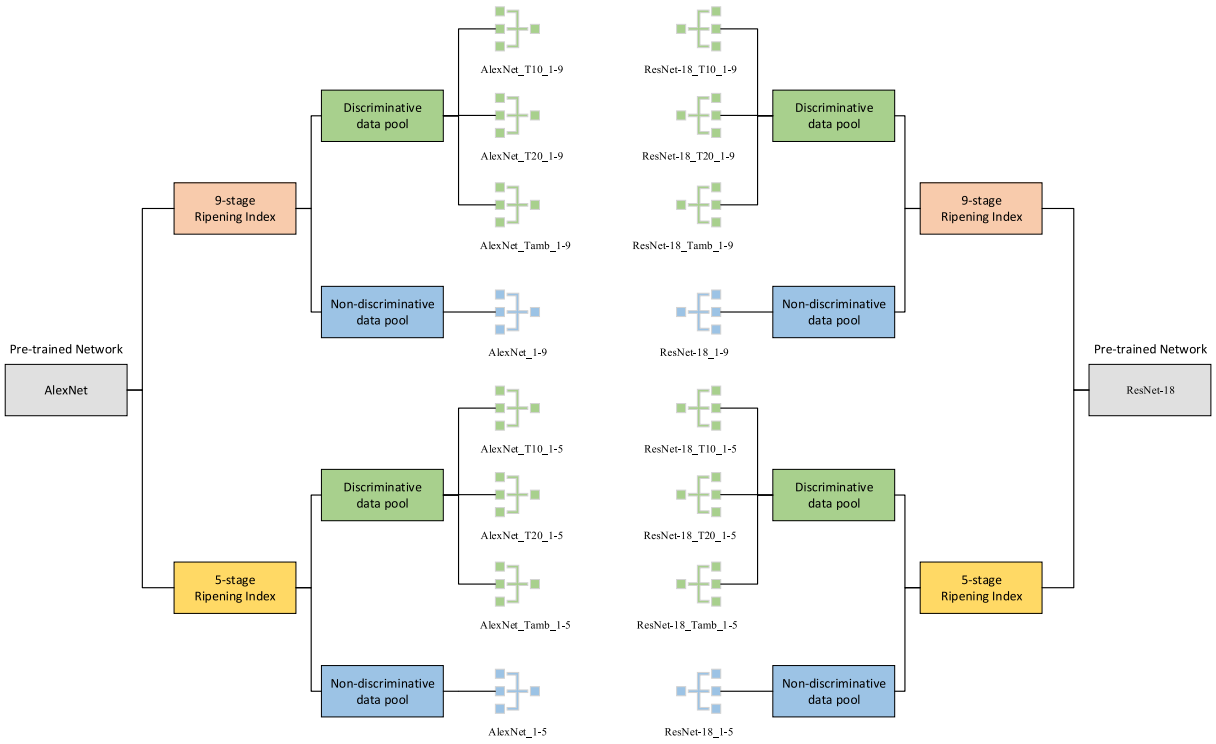

Figure 9 - Scheme representing all trained networks.

To accommodate each network's design to the characteristics of the new type of labelled data they would be training with, two of their original layers were altered. The third-to-last layer was replaced by a *fully connected layer* with a number of outputs corresponding to the defined number of classifications of each model (five for the 5-stage Ripening Index and nine for the 9-stage one). The last layer was also replaced by a regular *classification layer*, to match its output size to the one of the previous layers.

Table i and **Table ii** show the layer architecture analysis for two examples of the designed networks, considering the pretrained models they were based on, AlexNet (**Table i**) and ResNet-18 (**Table ii**).

Each network was trained for a total of 30 epochs using a mini-batch size of 64 files. As the ResNet-18 base architecture is highly more complex than that of the AlexNet, its derived networks were trained using a constant learning rate of 0,01, whereas the networks based on the second used a slower constant learning rate of 0,001 to compensate for that difference. During this process, every 50 iterations would trigger a validation step, using images from a separate database, which is further detailed in **Figure 10**.

An example of the training scripts that were used can be found in **Appendix - Chapter I.I**.

4.5.2. Test and Validation

Each trained network was given a sample set of images and respective labels, all different from the ones used in its training, and with a dimension corresponding to 20% of the training data.

The accuracy results of both the test and validation sets of each trained network were used to compare their individual performances.

An example of the scripts that were written for the test and validation steps can be found in **Appendix - Chapter I.II**.

Figure 10 shows the flow of the whole process comprising the building of the database and its subdivisions, as well as the training, recurrent validation, and testing of the final model.

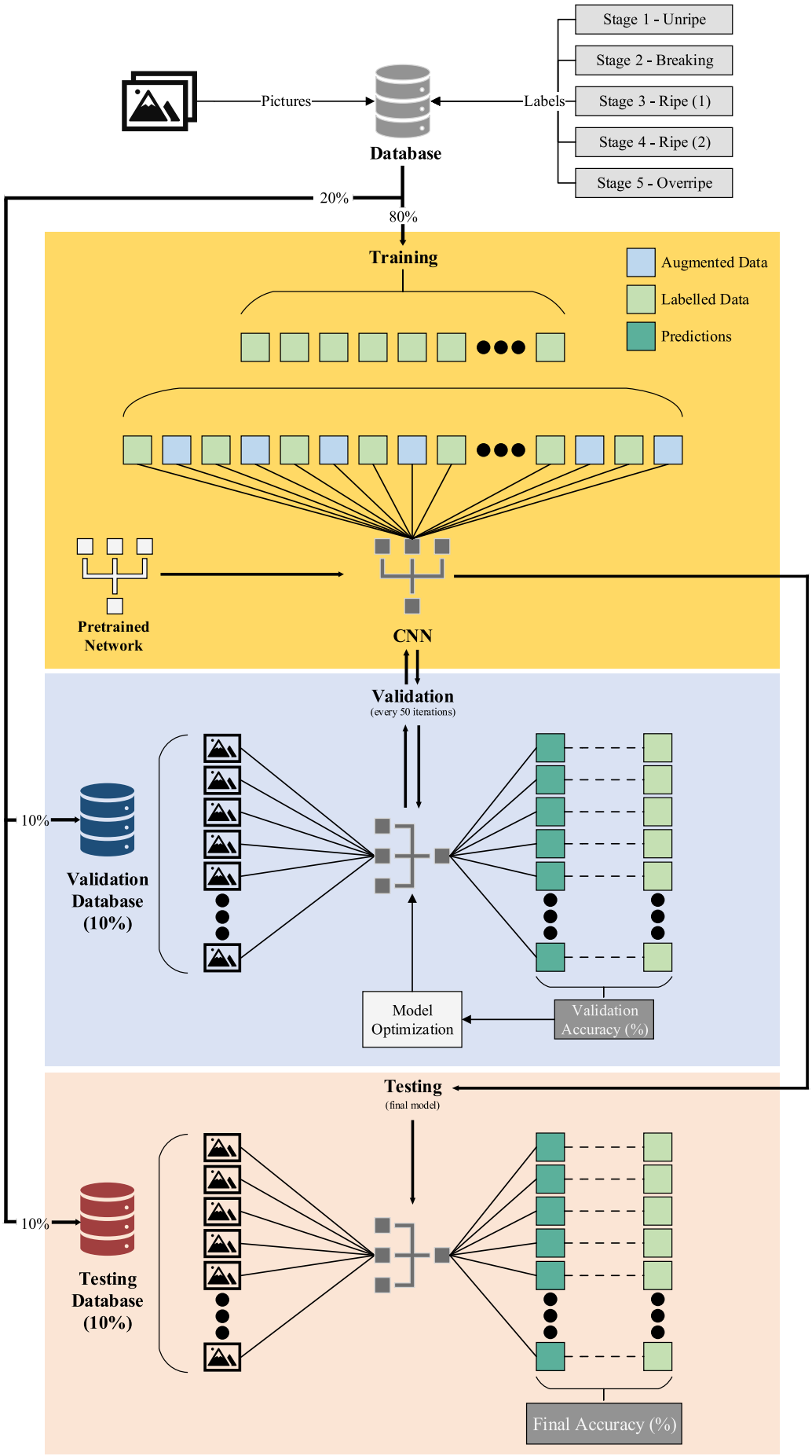

Figure 10 - Scheme representing the building process of the trained CNNs.

5. Results and Discussion

5.1. First Observations

The 2021/2022 winter was the fourth hottest in Portugal since 1931, with the highest average maximum temperature of the last 90 years. It was also the fifth driest winter in the same period, with only 33% of the average precipitation normally experienced during this time of the year. The region of Algarve was one of the most affected, reaching situations of severe to extreme drought between December 2021 and February 2022 (Instituto Português do Mar e da Atmosfera, 2022).

This was one of the restraints pointed out by the avocado fruit supplier, as it rushed the maturation of the fruits, which were already reaching their higher marketable levels of dry matter content when the experiment started.

Many of the samples exhibited marks of wind rub damage, caused by abrasion of the skin from branches or leaves, and some of them had marks of sunburn damage, probably related to the aforementioned weather conditions.

5.1.1. Calibre

According to the United Nations Economic Commission for Europe (UNECE) Standard FFV-42, concerning the marketing and commercial quality control of avocado fruits, the following table (**Table 2**) summarizes the weight and calibre of the used samples (UNECE, 2017):

Table 2 - Size observations of the avocado fruit samples.

		Calibre Code
Number of Samples	478	-
Maximum Weight	366g	10
Minimum Weight	133g	30
Median Weight	189g	22
Standard Deviation	47g	-

5.1.2. Initial Dry Matter Content

The initial dry matter (DM) content of the avocado fruits used in the experiment is an indicator of their pre-harvest maturity and has a direct impact on the ripening process.

From the eight samples that were assessed for their initial dry matter, the results indicate an average of 34% DM, with a standard deviation of 2,8%. All analysed samples fell in between 31% DM and 39% DM, which are considered high for industry standards, which usually recommend avocado fruits to be harvested when they are between 25% DM and 30% DM (Carvalho et al., 2014), indicating that the avocado fruits used in this study were harvested at a higher maturity stage than what is usual among avocado suppliers.

These findings seem to be related the previously discussed atypical weather conditions and suggest that the avocados used in the experiment might go through an accelerated ripening process and be more susceptible to physiological disorders and mechanical damage (Wu et al., 2011).

The maturity of the fruits included in the experiment might be a key factor to account for when using the trained networks to make predictions for avocados of different sources and conditions, since they would likely express a different ripening behaviour. Ideally, more sets of labelled data should be collected from different regions, cultivars, and harvesting years, so that the specific traits of each growing environment would be diluted in a more diverse data pool, which would expectedly produce more accurate predictions.

5.2. Heterogeneity of Ripening

As the degree of variation in the ripening process of the avocado fruits can be a challenge for the visual assessment of their Ripening Index stage (see **Chapter 2.2.2**), the heterogeneity of the attributed classifications along the research can be a good indicator of the potential accuracy of this system. The following paragraphs aim to study these variations, in a boxplot format, to better visualize the discrepancies of the controlled ripening process.

5.2.1. T10 Group

The sample group that was stored at 10 °C and 85% RH experienced a slower progression of the traits associated with the ripening process. The following boxplot (**Figure 11**) shows the evolution of the Ripening Index classifications from the samples along the daily assessments, for a total duration of 28 days.

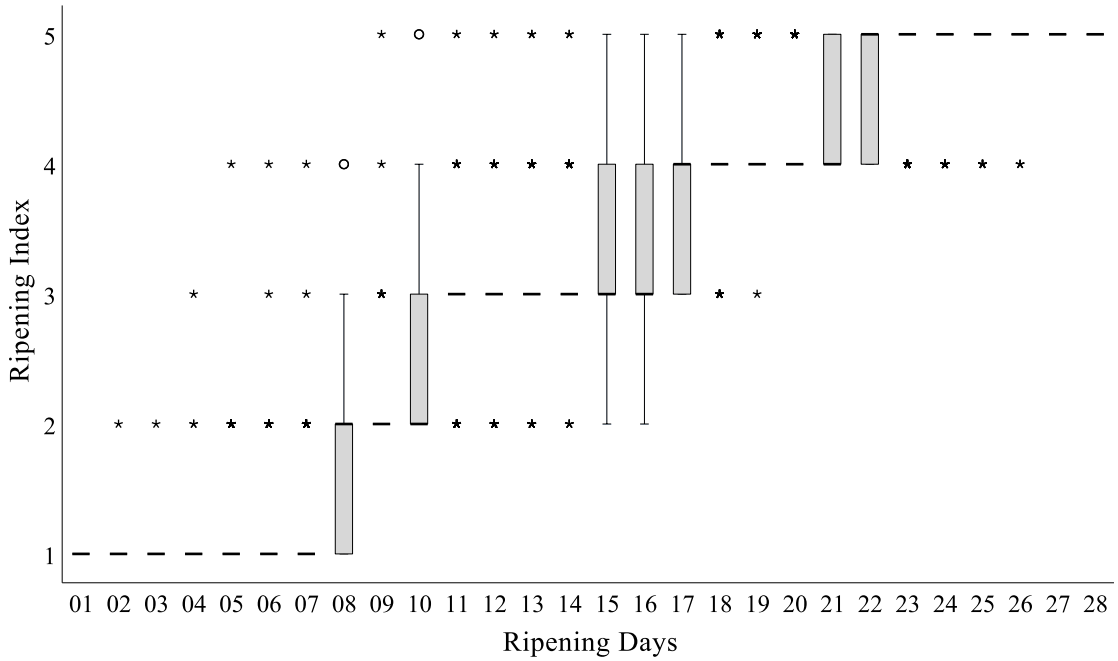

Figure 11 - Ripening heterogeneity for the T10 sample group.

Apart from the samples recognized as mild and extreme outliers, marked with the round and star shapes, respectively, the group took about 7 days to start showing signs of transition into the ripe stages. From the eighth day onward, a higher variance among the attributed classifications becomes more evident, suggesting that the mid stages of the Ripening Index are the ones where predicting the exact ripeness of the fruit becomes more of a challenge.

Although some outliers reached full apparent ripeness after around 10 days, it was only from the third week of the process that this became a trend among most group samples, that were all showing evident signs of senescence by the fourth week of the experiment.

5.2.2. T20 Group

The samples that were stored at a controlled atmosphere of 20°C and 85% RH started to show apparent signs of ripening right from the first days of the experiment. They also took a significantly shorter time to achieve the ripe stages, and the subsequent first signs of senescence and spoilage. For these reasons, the daily collection of data from this group took only half the time of what happened with the T10 storage group, as by the end of the second week, all samples were classified as overripe or spoiled.

The following boxplot (**Figure 12**) represents the evolution of the attributed classifications for the samples of this group throughout the duration of the experiment.

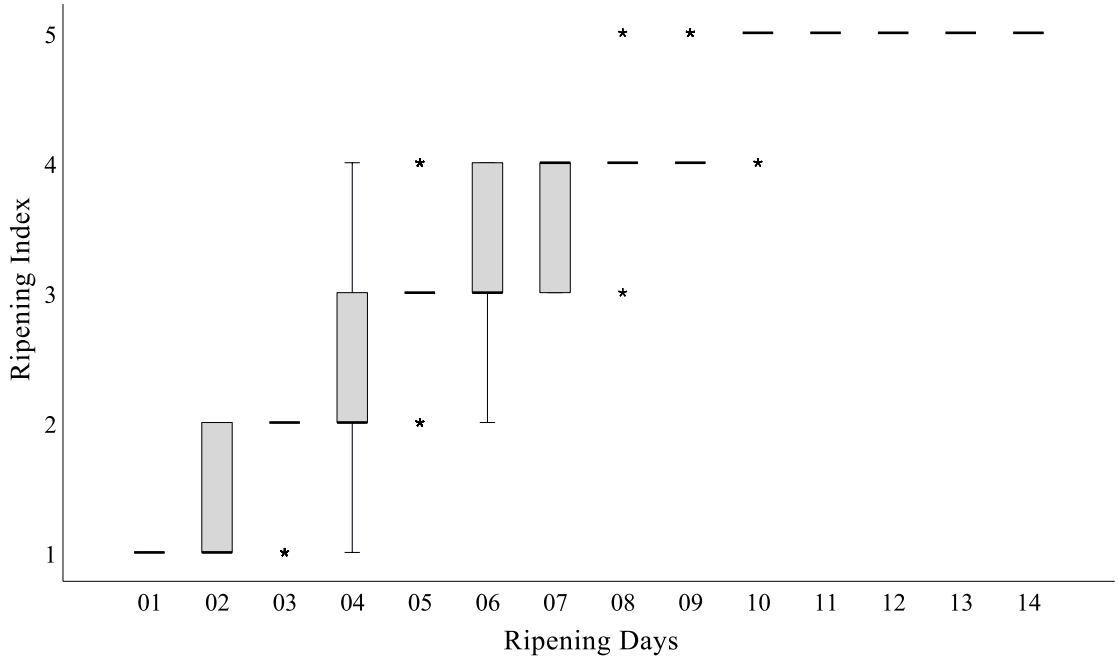

Figure 12 - Ripening heterogeneity for the T20 sample group.

As there were already fruits in the transition stage by the second day of the experiment, which corresponded to the fifth day of post-harvest, the heterogeneity of the classifications can be noticed from the start, unlike the T10 group where it was mostly evident in the mid stages of the experiment. Once again, the range of attributed labels goes as far as two stages apart, with the exception of day 4, where some outlier samples were still apparently unripe, while others were already showing signs of full ripeness.

5.2.3. Tamb Group

Although the samples from the Tamb group were not stored at a controlled environment, their apparent behaviour was not much different than the ones from the T20 group. Although there were some oscillations in temperature registered along the duration of storage, it averaged at 18,7°C, which was probably not distinct enough to the conditions experienced by the controlled environment group to produce noticeable differences in the ripening trend of the samples.

Figure 13 shows the fluctuations in storage temperature for the Tamb storage group, that oscillated between a registered minimum of 15,8°C and a maximum of 21,7°C, with a variance of 1,4°C.

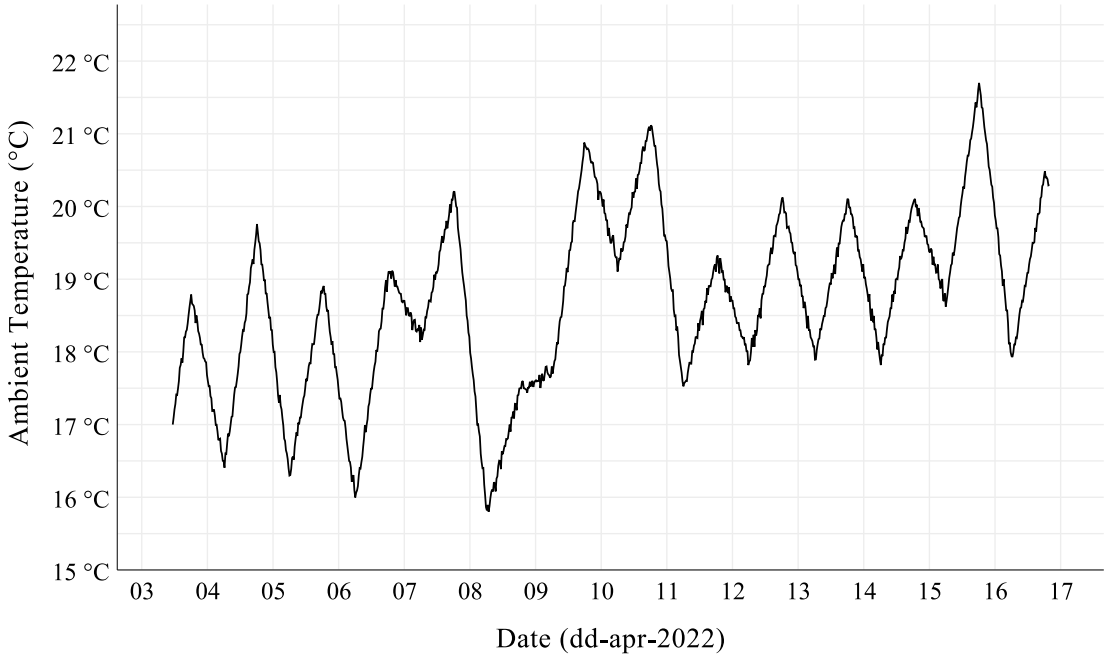

Figure 13 - Fluctuations in ambient temperature for the Tamb storage group.

Due to a technical error, it was not possible to retrieve the results for the oscillations in ambient humidity, which could have added another layer of analysis for the Tamb group.

When analysing the evolution of the classification labels of the Tamb group along the duration of the experiment (**Figure 14**), it becomes noticeable that this ample group experienced a very similar evolution trend to the T20 group, with signs of ripeness starting to show right from the start of the experiment and a similar degree of variance in range among the mid stages, culminating in the first signs of senescence from the beginning of the second week of storage.

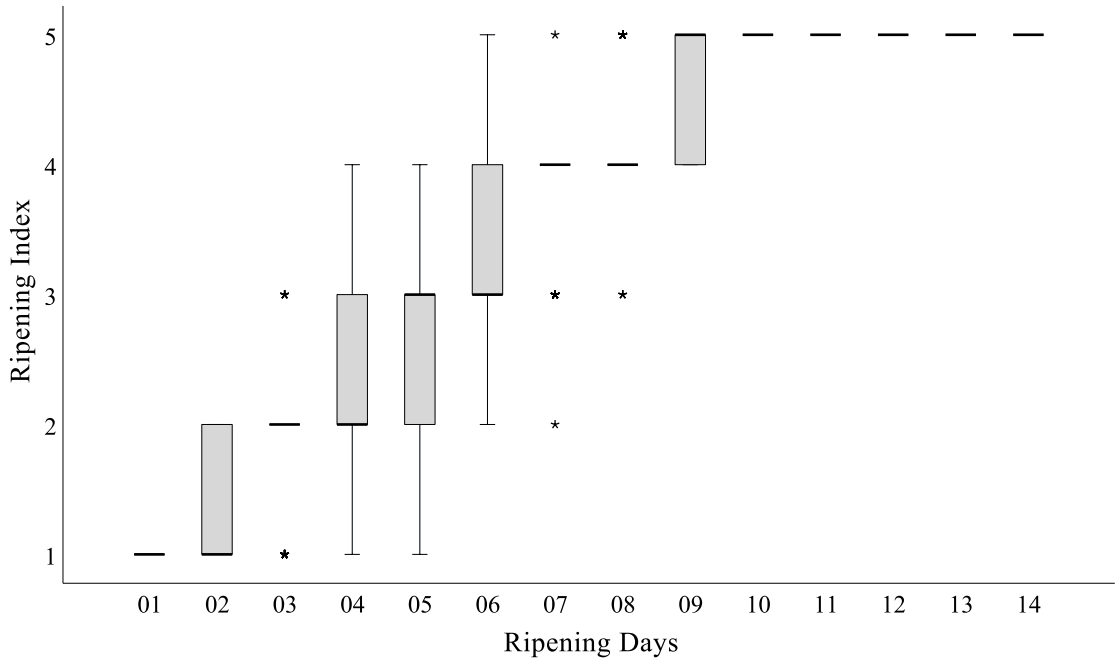

Figure 14 - Ripening heterogeneity for the Tamb sample group.

Overall, the boxplots show an evident heterogeneity along the ripening process, with different fruit samples that were subject to the same storage conditions presenting daily discrepancies in their Ripening Index classifications that, in extreme cases, can go up to three stages in the 1-5 stage format.

These variations are more apparent within the mid stages (2-4) of the index, and can, in part, be linked to differences in the pre-harvest maturity of the fruits, which have been previously assessed in the initial dry matter studies. But they also show that the ripening process of the avocado fruit is somewhat uneven and difficult to fully control.

Also, with the ripening index being assessed by a trained panel of researchers, it was subject to human error, which can also amplify the heterogeneity of the classifications.

When comparing the results from the different storage groups, all of them show a similar trend in what concerns to this heterogeneity, which suggests that it is not a result of the storage environment of the fruits, but rather from other factors such as their individual pre-harvest condition, or other unknown events within their biochemical profile.

Apart from the differences in the pace of the ripening process, there were also some noticeable differences in the pigmentation changes associated with ripeness. The avocados which ripened at a higher temperature developed an apparently stronger pigmentation, while the ones from the T10 group not only took longer to change colour, as most of them started to show signs of senescence while still unripe.

5.3. Mass Loss

Mass loss during the storage of avocado fruits is associated with quality degradation and is directly related to the transpiration rate and respiration rate of the samples. Though the first is the main contributor to this phenomenon, considering that the RH of both T10 and T20 remained the same, differences in mass loss between the two groups can be mostly attributed to their respiration rates, which have direct influence on the fruits ripening process (Lufu et al., 2019).

In all three storage groups, the mass loss occurred at a steady linear rate (**Figure 18**). This was expected for the two groups in controlled storage, but for the Tamb group, it suggests that the fluctuations of the ambient atmosphere (**Figure 13**) were not strong enough to cause a disruption in the transpiration and respiration rates.

5.3.1. T10 Group

The sample group that was stored at a lower temperature, also exhibited a lower mass loss per day than the other two groups, with an estimated loss rate of 0,62% ± 0,01% of the sample's initial mass, in a 95% confidence interval. The following plot (**Figure 15**) shows the daily mass loss for the ten control samples of this group, presented in the form of the fraction of their initial weight.

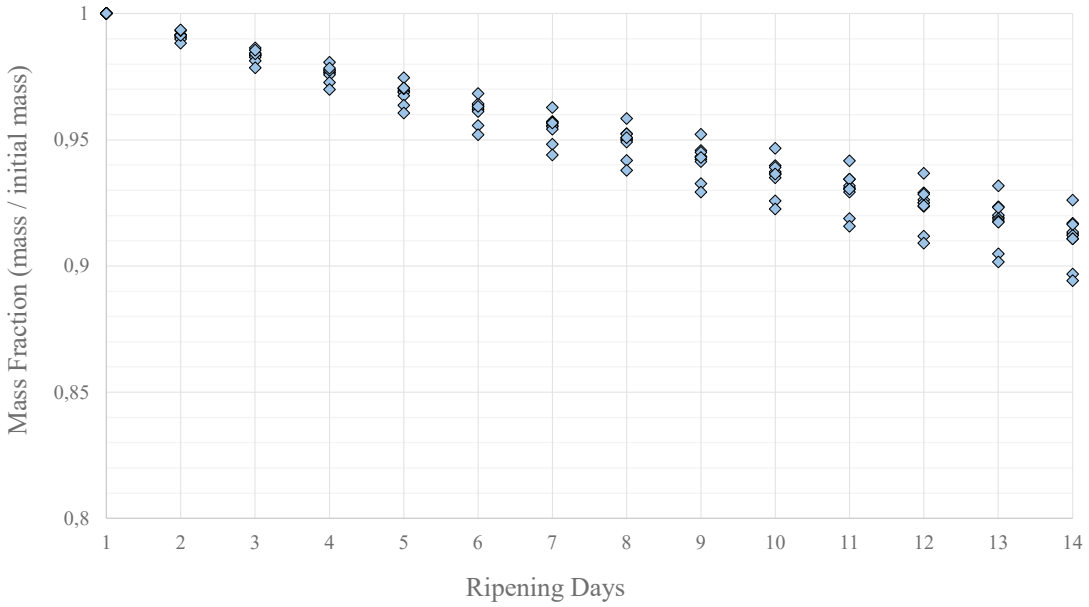

Figure 15 - Mass loss for the T10 sample group.

The studied samples of this group lost an average of 28,60g over the course of the 28 days of the experiment, which corresponds to about 17,4% of their average initial mass.

5.3.2. T20 Group

The samples that were stored within a controlled environment of 20°C and 85% RH went through a higher average mass loss per day than the ones stored at a lower temperature. **Figure 16** shows the daily mass loss for the ten controlled samples of the T20 storage group, in the form of fraction of their initial mass.

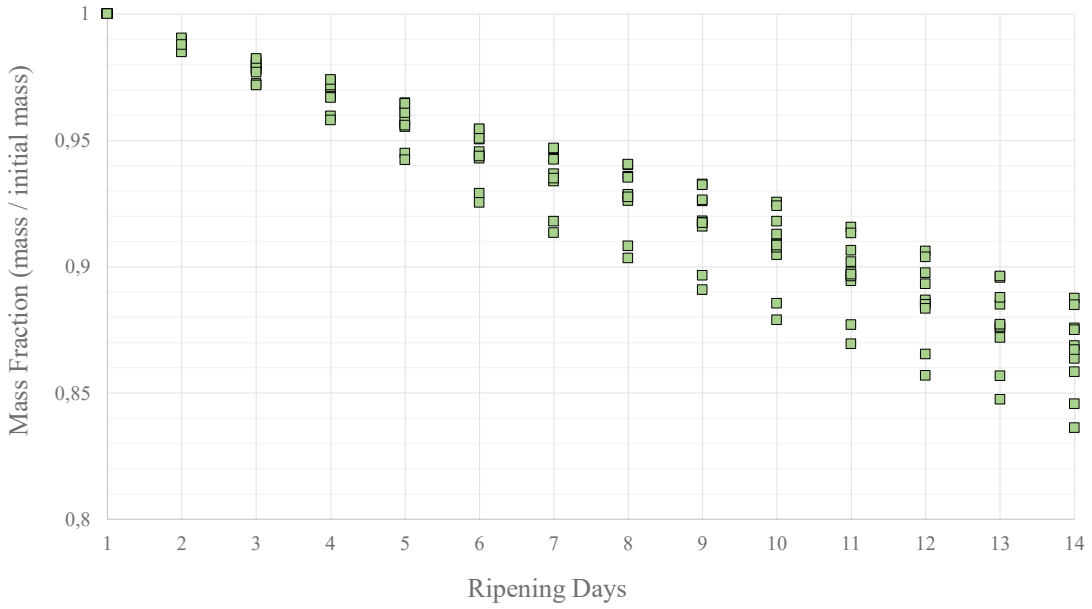

Figure 16 - Mass loss for the T20 sample group.

Although the average estimates point to a daily mass loss of 1,02% ± 0,05% at a 95% confidence interval, a value which is higher than the one of the T10 sample group, the avocados in this storage group took about half the time to reach full ripeness, making it so the average total mass lost in the process is of a lower value, corresponding to 23,29g, or around 14,0% of their initial mass.

This might suggest that the fruits retain more quality when ripened in these conditions, as the higher mass loss per day is compensated by the shorter ripening period.

5.3.3. Tamb Group

The group that was stored at ambient temperature exhibited the highest mass loss results among the three studied groups. Nevertheless, the linear regression of its values is about as strong as the other ones, suggesting that the linearity in the loss of mass was not affected by the oscillations in the environmental conditions such as temperature and relative humidity.

Estimates indicate that in these conditions, the samples lose 1,12% ± 0,04%, at a 95% confidence interval. The following plot (**Figure 17**) describes the results for the average mass loss of the ten control samples of this group.

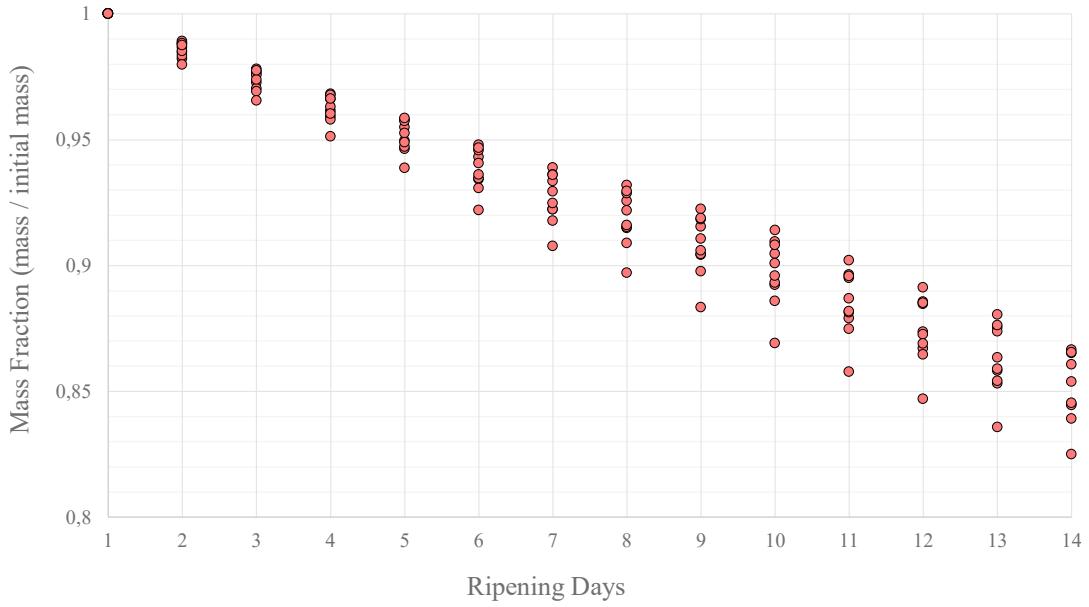

Figure 17 - Mass loss for the Tamb sample group.

Following the same trend as the T20 group, the fact that the samples took half the time to achieve the last stages of ripening made it so that the total mass loss was, on average, lower than the one of the T10 group samples, at about 15,5% of their initial mass, to an average total of 25,41g lost per sample.

Figure 18 - Comparative plot of the linear regression of mass loss between sample groups.

Figure 18 shows the linear regression of each sample group, for a better comparison of their behaviours.

Previous studies in the mass loss of avocado pears subject to different storage conditions point out to a similar behaviour to the one verified above (Sfishta, 2021), which suggests that this factor might not be directly influenced by the pre-harvest management of the fruit, including its harvest maturity, but rather a consequence of the fruits storage environment.

When comparing the results, it becomes apparent that a controlled environment is the optimum choice for retaining the most quality in avocado fruits, as the T10 sample group achieved the lowest results for mass loss per day, and the T20 resulted in the lowest total mass lost, on average. Opting between these two storage environments might depend on the expected storage time for the avocados, among other factors associated with their final quality.

5.4. Textural Analysis

Considering that both the skin and the flesh of avocado fruits experience relevant changes during their ripening process, a study of both the bioyield point and the average flesh firmness of the avocado samples was conducted in parallel with the image collection and Ripening Index classification, in the attempt to establish a correlative relation between the textural data, and the attributed labels.

5.4.1. Bioyield Point

The bioyield point is the maximum force exerted by a perforating probe before the skin is punctured, and it provides feedback on the resistance of the exocarp as the first protective layer of the inside's flesh (Bourne, 2002). The following plot (**Figure 19**) represents the distribution of the bioyield point of the studied samples, according to the attributed Ripening Index classifications, and their storage group.

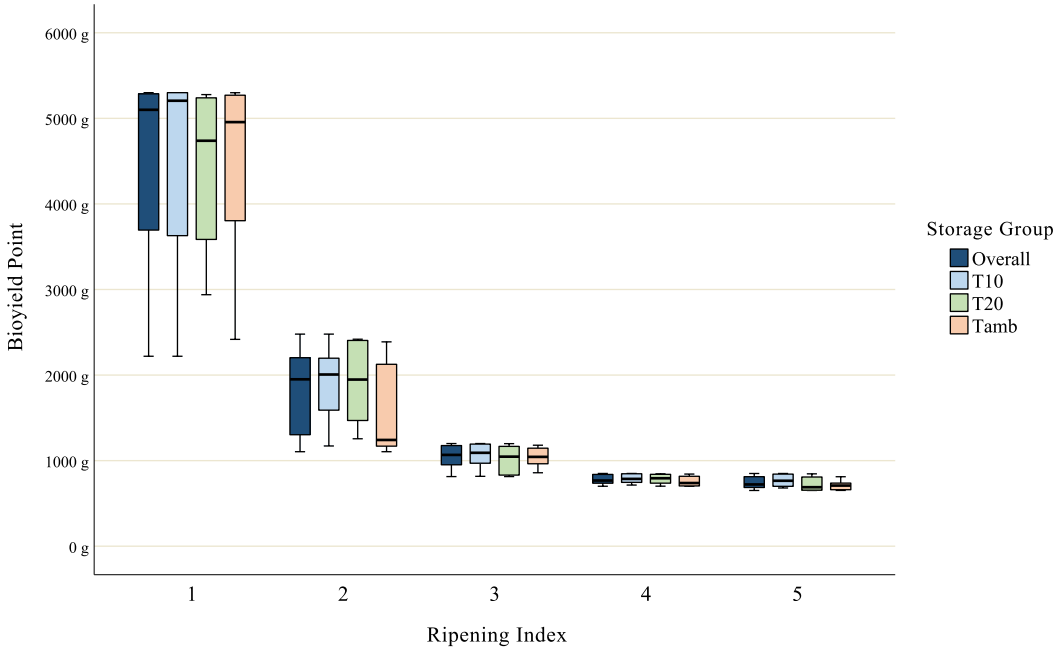

Figure 19 - Boxplot of the bioyield point for the 5-stage Ripening Index, by storage group.

The samples classified with the first two stages of the Ripening Index experienced a significantly larger variation in their bioyield point, as these correspond to the transition stages between the unripe fruits and the point where they start to be suitable for consumption.

Between the ripening classifications of 3 and 4 there was only a slight reduction in the bioyield point results, which is an indicator that these phases are much harder to distinguish and subsequently to classify.

The effects of senescence, starting to take place in the end of the fruit's shelf life, include a certain hardening of the skin due to the loss of water, but these were not noticeable in the test results, as they probably don't offer greater resistance to puncture, but rather a smaller displacement due to loss of flexibility.

5.4.2. Flesh Firmness

Changes in the flesh firmness are probably the most relevant textural changes induced by the ripening process of avocados, as they directly affect the edible portion of the fruit and its resulting quality. Ripe avocado flesh should be of a soft, almost spreadable nature, although for some applications, namely those which require the fruit to be sliced, a certain degree of flesh integrity is important (Bourne, 2002).

Being able to trace these changes in a way that we can predict the firmness of the skin without the use of destructive methods is one of the hardest challenges for quality assessment of avocados, and one that could benefit from smart-data tools integration.

The following boxplot[3] (**Figure 20**) describes the changes in the average flesh firmness of the studied samples along the image collection process, and again sorts them by their attributed classifications and storage group.

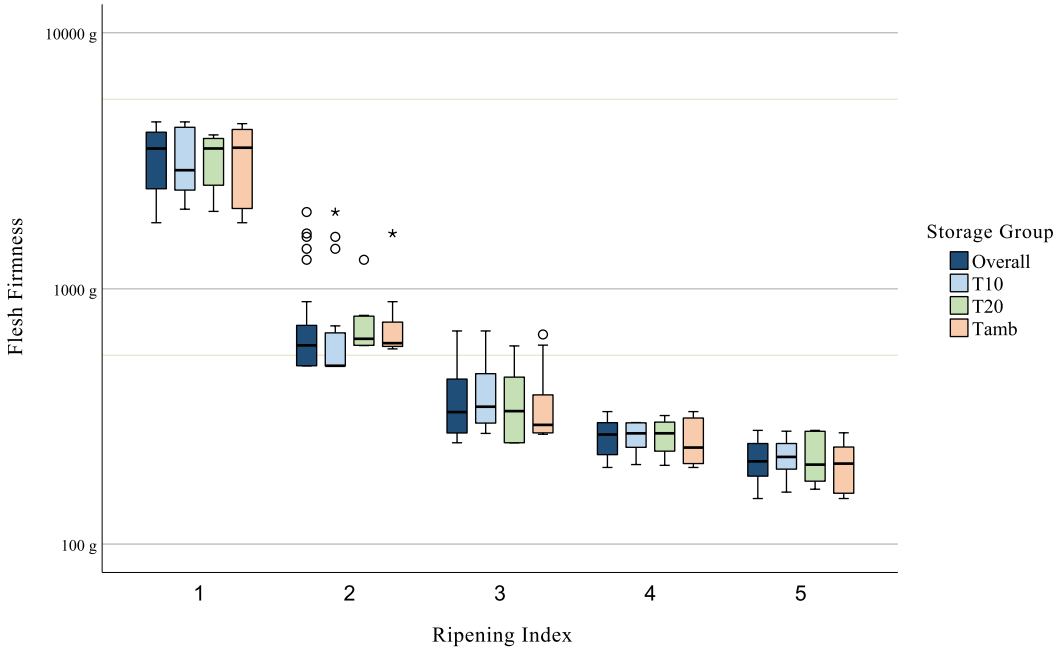

Figure 20 - Boxplot of the average flesh firmness for the 5-stage Ripening Index, by storage group.

[3] The Flesh Firmness axis is represented in a logarithmic scale.

The option for a logarithmic scale for the Flesh Firmness axis might conceal the perception of the drop in this value from the first stage to the transition phase, but it is the only way to present all results in the same plot without reducing the further stages to a very short visualization.

As it happened with the bioyield point results, the results of the samples classified as “unripe” were the ones with a higher degree of variation, coming up to the transition “breaking” stage. Once again, this corroborates the idea that the mid stages are the harder ones to trace.

Nevertheless, the average flesh firmness of the analysed samples continued to drop until the very last stage, as the continuous increase in oil content produces a softer flesh, which is usually more appealing for the final quality of the fruits, as described in **Chapter 2.2.1**.

5.4.3. Ripening Index Validation

Although the performed textural analysis did not influence the categorization of the samples, being a destructive method, the comparison between its results and the attributed classifications could be a good indicator of the accuracy of the latter.

Even considering the evident difference in pace for the ripening changes of the different storage groups, as it has been demonstrated in **Figure 11 toFigure** 14, the textural results indicate a similar behaviour for samples with the same Ripening Index classification.

Statistical analysis showed a negative Pearson correlation of -0,815, significant at the 0,01 level, between the bioyield point of samples, and their attributed Ripening Index classifications. When analysing the same for the flesh firmness results, data showed a negative Pearson correlation of -769, significant at the 0,01 level.

Also, one-way ANOVA didn’t demonstrate any significant differences both in the bioyield point and the flesh firmness results of samples classified with the same ripening stage.

These results suggest that the ripening assessment made daily by the trained panel of researchers to each sample was supported by an accurate characterization of the specific traits within each of the defined phases.

5.5. Network Training, Validation and Test

After gathering daily image data from the avocado fruits, each file was paired with its respective Ripening Index classification to build a labelled database. This database was then subdivided into different data pools, according to each network's objective. These pools comprised two different classification scales and either included all collected images or were sorted by the three different storage groups.

As shown in **Figure 10**, each data pool was split into three data sets. One used for the training stage, corresponding to 80% of the labelled images, one for the validation step and another for the final accuracy test, each corresponding to 10% of the data pairs.

The image files were renamed so that they would not carry any relevant information about their classification labels, as these were included in their parent folders.

Considering that each of the used pre-trained networks accepts an image input size of specific dimensions, all the training, validation, and test processes started with a resizing step, where a temporary pool was built according to the size criteria of the relevant network, as follows:

Table 3 - Image size for each CNN base model.

Pre-trained Network	Image Width	Image Height
AlexNet	227 pixels	227 pixels
ResNet-18	224 pixels	224 pixels

5.5.1. Conversion to a 9-Stage Ripening Index

As the ripening of the fruits and the changes that come with it is a continuous process, the Ripening Index classification is not always the most objective. Therefore, to mitigate human error, whenever an avocado was showing traits of two consecutive stages of ripening, an intermediate classification was assigned. This would later be converted to a 9-stage Index, with the five odd-numbered stages corresponding to the Ripening Index stages, and the remaining four even-numbered stages corresponding to the transition stages.

This extension of the classification stages should reduce the discrepancy between their sequential nature and the continuity of the ripening process, but it also produces a more complex data pool, as more ripening stages also mean less variation between them. Therefore, each network was trained with both sets of classifications and their results studied, to find out which one would produce the most accurate predictions.

5.5.2. Margin of Error

Considering the continuous nature of the ripening process, in contrast with the sequential nature of the Ripening Index, any visual assessment must be correlated to an occurrence probability, for which the use of a margin of error is recommended.

For the 5-stage index predictions, a fixed margin of error of ± 1 stage was used and compared with the exact-match results.

As for the 9-stage index predictions, the application of a ± 1-stage margin of error allowed to study how much the 5-stage model accuracy was affected by the transition stages, as it translates to an acceptable error of only half a stage when converted to that index. A margin of error of ± 2 stages was also studied for this dataset, as it can be directly compared to the ± 1-stage error margin of the 5-stage index.

5.5.3. Training Process

Each of the two built networks (AlexNet and ResNet-18) was trained with different data pools, to study the accuracy of its predictions according to multiple factors. A non-discriminative pool included image files from all storage temperatures and a set of labels from the 5-stage Ripening Index. A second non-discriminative pool included the same set of image files, but the corresponding labels were converted to a 9-stage index.

As the results of the non-discriminative pools with the 9-stage index produced the best results, the same classification method was used to train both networks with sets of data corresponding to each of the three storage groups.

5.5.4. Test and Validation

The validation procedures allow for an unbiased evaluation of the trained model by using a new set of labelled data while still performing hyperparameter optimization. Finally, the testing step should provide an unbiased evaluation of the final model performance (**Figure 10**).

The accuracy results of the final validation and test can be found in **Table 4 toTable** 9.

5.6. Final Accuracy Results

Table 4 comprises the final results for the networks trained with unrestrictive datasets, that included images of avocados ripen at each of the three storage environments.

Table 4 - Final accuracy results for the non-discriminative data pool.

Pretrained Network	Storage Group	Ripening Index	Margin of Error	Validating Accuracy	Final Accuracy
AlexNet	Non-discriminative	5 Stages	None	77,96%	75,07%
ResNet-18	**Non-discriminative**	**5 Stages**	**None**	**83,11%**	**79,41%**
AlexNet	Non-discriminative	5 Stages	1 Stage	98,00%	95,88%
ResNet-18	Non-discriminative	5 Stages	1 Stage	95,54%	96,37%
AlexNet	Non-discriminative	9 Stages	None	58,33%	55,24%
ResNet-18	Non-discriminative	9 Stages	None	60,47%	59,89%
AlexNet	Non-discriminative	9 Stages	1 Stage	87,39%	84,51%
ResNet-18	**Non-discriminative**	**9 Stages**	**1 Stage**	**92,81%**	**91,36%**
AlexNet	Non-discriminative	9 Stages	2 Stages	94,49%	92,70%
ResNet-18	Non-discriminative	9 Stages	2 Stages	97,13%	96,68%

Table 5 toTable 7 resume the final results of the networks that were trained with a discriminative data pool, in an attempt to assess the performative differences compared to the ones already shown in **Table 4**.

Table 5 - Final accuracy results for the T10 data pool.

Pretrained Network	Storage Group	Ripening Index	Margin of Error	Validating Accuracy	Final Accuracy
AlexNet	T10	5 Stages	None	78,45%	81,67%
ResNet-18	**T10**	**5 Stages**	**None**	**83,41%**	**84,16%**
AlexNet	T10	5 Stages	1 Stage	92,46%	91,86%
ResNet-18	T10	5 Stages	1 Stage	98,06%	95,25%
AlexNet	T10	9 Stages	None	57,54%	64,47%
ResNet-18	T10	9 Stages	None	67,67%	71,49%
AlexNet	T10	9 Stages	1 Stage	90,30%	91,63%
ResNet-18	**T10**	**9 Stages**	**1 Stage**	**96,55%**	**94,57%**
AlexNet	T10	9 Stages	2 Stages	94,18%	95,25%
ResNet-18	T10	9 Stages	2 Stages	97,84%	96,15%

Table 6 - Final accuracy results for the T20 data pool.

Pretrained Network	Storage Group	Ripening Index	Margin of Error	Validating Accuracy	Final Accuracy
AlexNet	T20	5 Stages	None	65,88%	73,05%
ResNet-18	**T20**	**5 Stages**	**None**	**72,30%**	**78,25%**
AlexNet	T20	5 Stages	1 Stage	98,65%	94,80%
ResNet-18	T20	5 Stages	1 Stage	97,30%	94,48%
AlexNet	T20	9 Stages	None	52,03%	58,12%
ResNet-18	T20	9 Stages	None	53,72%	64,94%
AlexNet	T20	9 Stages	1 Stage	87,50%	83,44%
ResNet-18	**T20**	**9 Stages**	**1 Stage**	**92,23%**	**87,98%**
AlexNet	T20	9 Stages	2 Stages	95,94%	92,21%
ResNet-18	T20	9 Stages	2 Stages	98,99%	96,75%

Table 7 - Final accuracy results for the Tamb data pool.

Pretrained Network	Storage Group	Ripening Index	Margin of Error	Validating Accuracy	Final Accuracy
AlexNet	Tamb	5 Stages	None	70,81%	73,99%
ResNet-18	**Tamb**	**5 Stages**	**None**	**82,89%**	**76,69%**
AlexNet	Tamb	5 Stages	1 Stage	88,59%	93,92%
ResNet-18	Tamb	5 Stages	1 Stage	93,62%	92,91%
AlexNet	Tamb	9 Stages	None	59,73%	56,08%
ResNet-18	Tamb	9 Stages	None	62,42%	58,78%
AlexNet	**Tamb**	**9 Stages**	**1 Stage**	**82,56%**	**87,50%**
ResNet-18	Tamb	9 Stages	1 Stage	86,58%	86,49%
AlexNet	Tamb	9 Stages	2 Stages	91,61%	96,28%
ResNet-18	Tamb	9 Stages	2 Stages	94,30%	94,26%

Table 8 compiles the information on the previous four tables, in order to compare the impact of the Ripening Index model (5 stages versus 9 stages).

Table 8 - Average final accuracy for each Ripening Index model.

Pretrained Network	Ripening Index	Margin of Error	Final Accuracy	
AlexNet	5 Stages	None	75,95%	**77,79%**
ResNet-18	5 Stages	None	79,63%	
AlexNet	5 Stages	1 Stage	94,12%	**94,43%**
ResNet-18	5 Stages	1 Stage	94,75%	
AlexNet	9 Stages	None	58,48%	**61,13%**
ResNet-18	9 Stages	None	63,78%	
AlexNet	9 Stages	1 Stage	86,77%	**88,44%**
ResNet-18	9 Stages	1 Stage	90,10%	
AlexNet	9 Stages	2 Stages	94,11%	**95,04%**
ResNet-18	9 Stages	2 Stages	95,96%	

Finally, the results of all trained networks are compiled and summarized in **Table 9**, for an overall perspective of the accuracy results across the different models.

Table 9 - Summary of the overall final accuracy results.

Pretrained Network	Average Final Accuracy		
	Non-discriminative data pool	Discriminative data pool	Overall
AlexNet	80,68%	82,28%	**81,88%**
ResNet-18	84,74%	84,88%	**84,84%**
Both Networks	**82,71%**	**83,58%**	**83,36%**

Despite the differences in architecture and complexity between each of the two pre-trained networks, both achieved similar results across all groups and classification models, with a slight advantage for the ResNet-18 based networks.

While the extension of the Ripening Index model translates in a lower degree of variance in recognizable visual traits between each stage, which could eventually add unnecessary complexity to the training of the networks, the implementation of the 9-stage model allowed to define a margin of error of only half a stage of the initial 5-stage model, which couldn't be assessed otherwise.

When directly comparing the 5-stage index exact-match results with the corresponding 9-stage model ones, the former achieved a higher accuracy. Nevertheless, the application of the 1-stage margin of error for the 9-stage classifications resulted in a significant increase in accuracy, making it a very plausible solution in order to obtain predictions that still point to a limited region of the Ripening Index, but that account better for the transitional variance in between each of its stages.

Taking the practical example of the ResNet-18 results from the non-discriminative data pools (**Table 4**), the networks trained with the 5-stage model only achieved better results when no margin of error was applied, with an accuracy of 79,41% against the 59,89% of the 9-stage model. From the former, 96,37% of the predictions fell within a 1 stage margin, while the latter predicted correctly 96,68% of the images within a similar region (± 2 stages). But the 91,36% correct predictions from the 9-stage network with only a 1-stage margin are what stands out from this methodology, as they suggest that the network can correctly identify the Ripening Index of the assessed samples, with a degree of precision of only half a stage.

Comparing the results of the networks trained with data from a single storage group, with the ones that were given a non-discriminative dataset (**Table 8**), there is no relevant difference in the obtained accuracy, which could indicate that the networks were capable of distinguish the particular traits related with the ripening stage of the samples and weren't affected by the different manifestations that were related to the storage environment.

It's worth noting that from the discriminative data pools, T10 group was the one that produced the most accurate results, with even a slight advantage to the non-discriminative sets. This could be explained by the larger amount of data it produced, as its ripening process took double the amount of time of the other two groups, and therefore resulted in a dataset twice as large, which could be key to a more diverse set that results in better training.

Considering the data pool size is an important factor for achieving the best results when training CNNs, as having a diverse input is essential to train the network on recognizing each particular trait, the networks trained with the T20 and Tamb data pools would benefit from a larger set of data. Looking backward, as they showed a very similar trend in the progression of the ripening process, it would have probably served better to have joined them in the same set, which would expectedly produce even better results than the ones verified in this experiment.

Although the training process includes a recurrent validation step, the comparison of the validating accuracy to the final accuracy of the network allows us to rule out a possible overfitting of the training model to the validation set, as such would translate in a noticeable discrepancy between each of those values. This was not apparently verified among the trained CNNs, as all the validation accuracy results fall in the same region as the corresponding final accuracy results.

6. Conclusion

Improvements in the application of smart-data tools in the food industry require large amounts of data that can be channelled into their development. The creation of a labelled photographic database not only served as the foundation for this project, but most importantly, will allow for other exploratory studies that can use the gathered information to develop new and enhanced tools.

As all the avocados used in this study were sourced from the same region and harvested at the same time, there was a small degree of variation in what concerns to the pre-harvest properties of the fruits that directly impact their ripening behaviour. Nevertheless, this allowed for a better comparison of the post-harvest handling factors, as any behavioural differences between the sample groups could be attributed to the three different storage environments.

The use of classification labels to describe the evolution of the ripening factors in avocado fruits required the adaptation of a continuous process to a discrete function. The definition of a Ripening Index that comprised the five most relevant ripening stages, allowed for the categorization of the collected images, so that the built networks could look for common visual traits among each stage.

The recurrent textural analysis, which took place along with the image collection, was the most objective source of data, and served as a validator for the ripening assessment of the research team, achieving a strong correlation between the textural results and the attributed Ripening Index classifications across all storage groups, with no significant differences in between them, which was interpreted as a sign of coherence. This might be a consequence of the limited number of categories, with very distinct characteristics, but also of the high number of labelled samples, which diluted the impact of human error.

According to what was expected, the storage conditions of each group had a very noticeable effect on the ripening process, which was about twice as fast for the avocados stored at 20 °C and at ambient temperature, when compared to those stored at 10 °C. The visual changes experienced by the fruits during this process were also different, as the fruits stored at higher temperatures developed their characteristic purplish pigmentation before any signs of senescence were noticed, which was not always the case for the fruits that had a longer ripening time frame.

Even within each storage group, there was a relevant degree of variation in the progression of the Ripening Index classifications. This might be partially related to human error in the visual assessment of the samples, but it was mostly attributed to the well-documented heterogeneity that characterises the evolution of the ripening factors in avocado fruits, which makes them hard to trace. While this can be a challenge for the development of smart-data tools that accurately track these changes, it also reinforces the idea that taking use of the computational power of Artificial Neural Networks might be the approach that better serves their comprehension.

From the perspective of the project's scope, it became evident that to build a network capable of recognizing all these visual traits, it's important to build a solid database, comprising as many samples as possible and subject to different scenarios, so that ultimately the tool can pick up the specific behavioural traits that result from the multiple factors with direct influence on the ripening process of avocado fruits. Nonetheless, the results from the designed networks did not show an apparent loss of accuracy when trained with non-discriminative data sets comprising images from all the storage groups, which suggested that the networks could pick up the individual traits that are characteristic of the ripening stage of the fruit and not directly affected by its storage environment.

The conversion to a 9-stage index, that added four transitional stages to the 5-stage Ripening Index, proved to be an effective attempt to improve the accuracy of the predictions, as it allowed for the implementation of a 1-stage margin of error, corresponding to half of a stage from the initial index, and though it reduces the variation between each stage, which therefore makes their specific traits harder to trace and train to detect, it also provides a better description of the continuous changes that comprise the ripening process of avocado fruits.

The application of the transfer learning concept, which was the innovative foundation of this project also exhibited promising results, with both networks achieving a similar accuracy in their predictions, despite their differences in architecture and complexity.

The potential applications of smart-data tools capable of making predictions on perishable products' shelf-life and other quality-related factors are boundless and will benefit from further studies and different approaches. The results of this project should reinforce that path and show how much these tools could potentially change the food industry panorama.

7. Suggestions for Future Work

1. Train the network to recognize other quality features

The ripening process is one of the most important factors with direct influence on the final quality and shelf-life of avocado fruits. Nevertheless, other important features such as spots or marks on the skin surface, that can derive from wind rub damage, sunburn, disease, contamination, mechanical damage from post-harvest handling, and numerous other factors, can be easily evaluated by visual assessment, which indicate that they can be recognised by CNNs if properly trained with the relevant pairs of image and data.

2. Explore other smart-data tools

The scope of this project could be expanded by the creation of Computer Vision tools that could, for example, track in real-time the evolution of the ripening stages of a whole batch of avocados. These would have to clearly distinguish each fruit unit in the batch and apply the current knowledge to make an individual prediction that could use the batch average to reduce the individual prediction error.

3. Extend the study to other cultivars and proveniences

As there are multiple avocado cultivars with market prevalence, from numerous geographical sources that directly affect the pre-and post-harvest behaviour of the fruits, further studies with diverse sets of samples will allow for a better adaptation of the predictions to the practical requirements of the food industry.

4. Improve the Ripening Index

The definition of a Ripening Index derived from the need to create a sequential classification model that could integrate several factors associated with the ripening process of the avocado fruits. Despite the efforts to make it as objective as possible, the current model is still highly dependent on a visual assessment, and therefore exposed to human error. Improvements on this model could also produce more accurate predictions.

5. Study the application of these systems on other fruits and vegetables

Making use of the Transfer Learning concept, which served as the innovative base of this project, the knowledge of the trained networks could be used to achieve better results when extending its application to other fruits and vegetables, especially the ones where the shelf-life is hard to trace and highly dependent on the post-harvest ripening process.

Bibliography

Aerobotics. (2021). Produtores usam drones para fazer com que cada gota conte. *AgriTerra*, (4), 76-77.

Aggarwal, C. C. (2018). *Neural Networks and Deep Learning* (1st ed.). Springer International Publishing. https://doi.org/https://doi.org/10.1007/978-3-319-94463-0

Agrawal, R., Wankhede, V. A., Kumar, A., Luthra, S., Majumdar, A., & Kazancoglu, Y. (2021). An exploratory state-of-the-art review of artificial intelligence applications in circular economy using structural topic modeling. *Operations Management Research*. https://doi.org/10.1007/s12063-021-00212-0

AGROGES. (2021). *Estudo da importância da cultura do abacate na região do Algarve - Resumo Técnico* https://www.agroportal.pt/wp-content/uploads/2021/06/Abacate-na-Regi%C3%A3o-do-Algarve_Relat%C3%B3rio_Resumo-T%C3%A9cnico_v2.pdf

AOAC. (2000). *Official Methods of Analysis of AOAC International* (17th ed.). AOAC International Inc.

Arzate-Vázquez, I., Chanona-Pérez, J. J., Perea-Flores, M. d. J., Calderón-Domínguez, G., Moreno-Armendáriz, M. A., Calvo, H., Godoy-Calderón, S., Quevedo, R., & Gutiérrez-López, G. (2011). Image processing applied to classification of avocado variety 'Hass' (*Persea americana* Mill.) during the ripening process. *Food and Bioprocess Technology*, *4*(7), 1307-1313. https://doi.org/10.1007/s11947-011-0595-6

AZUD. (2021). Abacate: cultura de alto valor onde não se pode correr riscos. *AgriTerra*, (4), 88-89.

Barman, K., Ahmad, S., & Siddiqui, M. W. (2015). Factors Affecting the Quality of Fruits and Vegetables: Recent Understandings. In M. W. Siddiqui (Ed.), *Postharvest Biology and Technology of Horticultural Crops* (pp. 1-50). Apple Academic Press.

Bhuyan, M. K. (2020). Image Formation and Image Processing. In *Computer Vision and Image Processing Fundamentals and Applications* (pp. 1-60). CRC Press.

Blasco, J. (2012). Fruit, vegetable and nut quality evaluation and control using computer vision. In D.-W. Sun (Ed.), *Computer Vision Technology in the Food and Beverage Industries* (pp. 379-399). Woodhead Publishing.

Bost, J. B., Smith, N. J. H., & Crane, J. H. (2013). History, Distribution and Uses. In B. Schaffer, B. N. Wolstenholme, & A. W. Whiley (Eds.), *The Avocado: Botany, Production and Uses* (2nd ed., pp. 10-30). CAB International.

Bourne, M. C. (2002). Practice of Objective Texture Measurement. In *Food Texture and Viscosity* (2nd ed., pp. 189-234). Academic Press.

Broekman, A., & Steyn, W. J. (2021). smAvo: Packhouse optimization using smart avocadoes in South Africa. *Computers and Electronics in Agriculture*, *191*. https://doi.org/10.1016/j.compag.2021.106507

Broekman, A., Steyn, W. J., Steyn, J. L., Bill, M., & Korsten, L. (2020). smAvo and smaTo: A fruity odyssey of smart sensor platforms in Southern Africa. *HardwareX*, *8*, e00156. https://doi.org/10.1016/j.ohx.2020.e00156

Carvalho, C. P., Velásquez, M. A., & Van Rooyen, Z. (2014). Determination of the minimum dry matter index for the optimum harvest of 'Hass' avocado fruits in Colombia. *Agronomía Colombiana*, *32*(3), 399-406. https://doi.org/10.15446/agron.colomb.v32n3.46031

Ceelen, M. (2019). Data driven shelf life prediction.

Chakraverty, A., & Singh, R. P. (2014). Postharvest Management of Fruits and Vegetables. In *Postharvest Technology and Food Process Engineering* (pp. 315-356). CRC Press.

Cheng, J. H., Sun, D.-W., Nagata, M., & Tallada, J. G. (2016). Quality Evaluation of Strawberry. In D.-W. Sun (Ed.), *Computer Vision Technology for Food Quality Evaluation* (2nd ed., pp. 327-350). Academic Press.

Costa, J., Rosa, A., & Oliveira, P. (2018). Breve história, situação actual e perspectivas de futuro da cultura do abacateiro na região do Algarve. *Revista da APH*, (129), 33-36.

Cowan, A. K., & Wolstenholme, B. N. (2016). Avocado. In B. Caballero, P. M. Finglas, & F. Toldrá (Eds.), *Encyclopedia of Food and Health* (Vol. 1, pp. 294-300): Academic Press.

Cox, K. A., McGhie, T. K., White, A., & Woolf, A. B. (2004). Skin colour and pigment changes during ripening of 'Hass' avocado fruit. *Postharvest Biology and Technology*, *31*(3), 287-294. https://doi.org/10.1016/j.postharvbio.2003.09.008

Cruz, L., Pires-Ribeiro, J., & Barbosa-Póvoa, A. (2019). Design and Planning of Agri-Food Supply Chains. In *29th European Symposium on Computer Aided Process Engineering* (pp. 55-60). https://doi.org/10.1016/b978-0-12-818634-3.50010-2

Davies, C., & Böttcher, C. (2014). Other Hormonal Signals during Ripening. In P. Nath, M. Bouzayen, A. K. Mattoo, & J. C. Pech (Eds.), *Fruit Ripening: Physiology, Signalling and Genomics* (pp. 202-216). CAB International.

Duarte, A., Lopes, R., Furtado, J., & Duarte, J. (2018). Alguns aspectos da floração e vingamento do abacateiro. *Revista da APH*, (129), 29-32.

Duarte, J., Lopes, R., Furtado, J., Mogo, P., Mourinho, H., Reis, V., Sabbo, L., & Duarte, A. (2020). Dados preliminares de um estudo sobre produtividade e alternância em abacateiro (*Persea americana* Mill.), no Algarve. *Actas Portuguesas de Horticultura*(32), 238-244.

Ellen MacArthur Foundation. (2019a). *Artificial intelligence and the circular economy - AI as a tool to accelerate the transition*. http://www.ellenmacarthurfoundation.org/publications

Ellen MacArthur Foundation. (2019b). *Cities and Circular Economy for Food*.

Eurostat. (2022). *Crop production in EU standard humidity.* https://ec.europa.eu/eurostat/databrowser/view/APRO_CPSH1__custom_2968006/

FAO, IFAD, UNICEF, WFP, & WHO. (2022). *The State of Food Security and Nutrition in the World 2022. Repurposing food and agricultural policies to make healthy diets more affordable*. FAO. https://doi.org/10.4060/cc0639en

FAO, UNDP, & UNEP. (2021). *A multi-billion-dollar opportunity – Repurposing agricultural support to transform*

food systems.

Freire, E. (2021). Futuro passa por produzir com 'resíduo zero'. *AgriTerra*, (4), 78-83.

FRUITROP. (2021). *Avocado Consumption 2020* (European Avocado Market, Issue. https://www.fruitrop.com/en/Articles-by-subject/Review-and-Forecasts/2021/Avocado-Consumption-2020

Goodfellow, I., Bengio, Y., & Courville, A. (2016). *Deep Learning*. The MIT Press.

Graupe, D. (2013). *Principles of Artificial Neural Networks* (3rd ed., Vol. 7). World Scientific.

Grierson, D. (2013). Ethylene and the Control of Fruit Ripening. In G. B. Seymour, M. Poole, J. J. Giovannoni, & G. A. Tucker (Eds.), *The Molecular Biology and Biochemistry of Fruit Ripening*

(pp. 43-74). Wiley-Blackwell.

He, K., Zhang, X., Ren, S., & Sun, J. (2016). *Deep residual learning for image recognition* 2016 IEEE Conference on Computer Vision and Pattern Recognition (CVPR),

Hernández, I., Fuentealba, C., Olaeta, J. A., Lurie, S., Defilippi, B. G., Campos-Vargas, R., & Pedreschi, R. (2016). Factors associated with postharvest ripening heterogeneity of 'Hass' avocados (*Persea americana* Mill.). *Fruits*, *71*(5), 259-268. https://doi.org/10.1051/fruits/2016016

Hiwasa-Tanase, K., & Ezura, H. (2014). Climacteric and Non-climacteric Ripening. In P. Nath, M. Bouzayen, A. K. Mattoo, & J. C. Pech (Eds.), *Fruit Ripening: Physiology, Signalling and Genomics* (pp. 1-14). CAB International.

Hopkirk, G., White, A., Beever, D. J., & Forbes, S. K. (1994). Influence of postharvest temperatures and the rate of fruit ripening on internal postharvest rots and disorders of New Zealand 'Hass' avocado fruit. *New Zealand Journal of Crop and Horticultural Science*, *22*(3), 305-311. https://doi.org/10.1080/01140671.1994.9513839

Instituto Português do Mar e da Atmosfera, I. P. (2022). *Boletim Sazonal - Inverno 2021/2022*.

Kader, A. A. (2011). Postharvest biology of tropical and subtropical fruits. In E. M. Yahia (Ed.), *Postharvest biology and technology of tropical and subtropical fruits* (Vol. 1, pp. 79-111). Woodhead Publishing.

Kakani, V., Nguyen, V. H., Kumar, B. P., Kim, H., & Pasupuleti, V. R. (2020). A critical review on computer vision and artificial intelligence in food industry. *Journal of Agriculture and Food Research*, *2*. https://doi.org/10.1016/j.jafr.2020.100033

Krizhevsky, A., Sutskever, I., & Hinton, G. E. (2017). ImageNet classification with deep convolutional neural networks. *Communications of the ACM*, *60*(6), 84-90. https://doi.org/https://doi.org/10.1145/3065386

Kumar, I., Rawat, J., Mohd, N., Husain, S., & Khan, R. (2021). Opportunities of artificial intelligence and machine learning in the food industry. *Journal of Food Quality*, *2021*, 1-10. https://doi.org/10.1155/2021/4535567

Kumar, R., & Sharma, A. K. (2014). Ethylene Perception and Signalling in Ripening Fruit. In P. Nath, M. Bouzayen, A. K. Mattoo, & J. C. Pech (Eds.), *Fruit Ripening: Physiology, Signalling and Genomics* (pp. 193-201). CAB International.

LeCun, Y., Kavukcuoglu, K., & Farabet, C. (2010). Convolutional networks and applications in vision. *Proceedings of 2010 IEEE International Symposium on Circuits and Systems*, 253-256. https://doi.org/10.1109/ISCAS.2010.5537907

Lopes, M. V. (2021). Abacate pode trazer ao Algarve um contributo económico e social importante. *AgriTerra*, (4), 84-89.

Lu, Y., & Lu, R. (2016). Quality Evaluation of Apples. In D.-W. Sun (Ed.), *Computer Vision Technology for Food Quality Evaluation* (2nd ed., pp. 273-304). Academic Press.

Lufu, R., Ambaw, A., & Opara, U. L. (2019). The contribution of transpiration and respiration processes in the mass loss of pomegranate fruit (cv. Wonderful).

Postharvest Biology and Technology, *157*. https://doi.org/10.1016/j.postharvbio.2019.110982

Magwaza, L. S., & Tesfay, S. Z. (2015). A review of destructive and non-destructive methods for determining avocado fruit maturity. *Food and Bioprocess Technology*, *8*(10), 1995-2011. https://doi.org/10.1007/s11947-015-1568-y

Marvin, H. J., Janssen, E. M., Bouzembrak, Y., Hendriksen, P. J., & Staats, M. (2017). Big data in food safety: An overview. *Crit Rev Food Sci Nutr*, *57*(11), 2286-2295. https://doi.org/10.1080/10408398.2016.1257481

MathWorks. (2022a). *Deep Learning Toolbox - MATLAB*. https://www.mathworks.com/products/deep-learning.html

MathWorks. (2022b). *Design, visualize, and train deep learning networks - MATLAB*. https://www.mathworks.com/help/deeplearning/ref/deepnetworkdesigner-app.html

Miller, J. (2020). *Avocado: A Global History*. Reaktion Books.

Nayak, J., Vakula, K., Dinesh, P., Naik, B., & Pelusi, D. (2020). Intelligent food processing: Journey from artificial neural network to deep learning. *Computer Science Review*, *38*. https://doi.org/10.1016/j.cosrev.2020.100297

NobelPrize.org. (2022). *The Nobel Prize in Physiology or Medicine 1981* https://www.nobelprize.org/prizes/medicine/1981/press-release/

OECD/FAO. (2021). *OECD-FAO Agricultural Outlook 2021-2030*.

Osorio, S., & Fernie, A. R. (2013). Biochemistry of Fruit Ripening. In G. B. Seymour, M. Poole, J. J. Giovannoni, & G. A. Tucker (Eds.), *The Molecular Biology and Biochemistry of Fruit Ripening*

(pp. 1-20). Wiley-Blackwell.

Ozdemir, F., & Topuz, A. (2004). Changes in dry matter, oil content and fatty acids composition of avocado during harvesting time and post-harvesting ripening period. *Food Chemistry*, *86*(1), 79-83. https://doi.org/10.1016/j.foodchem.2003.08.012

Paluszek, M., & Thomas, S. (2020). *Practical MATLAB Deep Learning: A Project-Based Approach*. Apress. https://doi.org/10.1007/978-1-4842-5124-9

Pan, S. J., & Yang, Q. (2010). A survey on transfer learning. *IEEE Transactions on Knowledge and Data Engineering*, *22*(10), 1345-1359. https://doi.org/10.1109/tkde.2009.191

Ramadoss, T. S., Alam, H., & Seeram, R. (2018). Artificial intelligence and internet of things enabled circular economy. *The International Journal of Engineering and Science*, *7*(9), 55-63. https://doi.org/10.9790/1813-0709035563

Razavian, A. S., Azizpour, H., Sullivan, J., & Carlsson, S. (2014). *CNN Features Off-the-Shelf: An Astounding Baseline for Recognition* 2014 IEEE Conference on Computer Vision and Pattern Recognition Workshops,

Rohwer, J. G. (1993). Lauraceae. In K. Kubitzki, J. G. Rohwer, & B. V. (Eds.), *The Families and Genera of Vascular Plants* (Vol. II, pp. 366-391). Springer.

Scholz, M., & Kulko, R.-D. (2022). Dynamic pricing of perishable food as a sustainable business model. *British Food Journal*, *124*(5), 1609-1621. https://doi.org/https://doi.org/10.1108/BFJ-03-2021-0294

Seymour, G. B., & Tucker, G. A. (1993). Avocado. In G. B. Seymour, J. E. Taylor, & G. A. Tucker (Eds.), *Biochemistry of Fruit Ripening* (pp. 53-82). Springer Science + Business Media Dordrecht. https://doi.org/10.1007/978-94-011-1584-1

Sfishta, A. (2021). *Predictive modelling and Computer Vision Systems (CVS) for minimizing losses along avocado (Persea americana) fruit distribution chain* Universidade Católica Portuguesa].

Sood, S., & Singh, H. (2021). Computer vision and machine learning based approaches for food security: A review. *Multimedia Tools and Applications*, *80*(18), 27973-27999. https://doi.org/10.1007/s11042-021-11036-2

Stanford Vision Lab. (2020). *ImageNet Large Scale Visual Recognition Challenge (ILSVRC)*. https://image-net.org/challenges/LSVRC/

Subedi, P. P., & Walsh, K. B. (2020). Assessment of avocado fruit dry matter content using portable near infrared spectroscopy: Method and instrumentation optimisation. *Postharvest Biology and Technology*, *161*. https://doi.org/10.1016/j.postharvbio.2019.111078

Sutherland, A. B., & Kouloumpi, I. (2022). *More than Just SDG 12: How Circular Economy can Bring Holistic Wellbeing*. Retrieved Sep 8th 2022 from https://sdg.iisd.org/commentary/guest-articles/more-than-just-sdg-12-how-circular-economy-can-bring-holistic-wellbeing/

Torres-Sanchez, R., Martinez-Zafra, M. T., Castillejo, N., Guillamon-Frutos, A., & Artes-Hernandez, F. (2020). Real-time monitoring system for shelf life estimation of fruit and vegetables. *Sensors (Basel)*, *20*(7). https://doi.org/10.3390/s20071860

UNECE. (2017). UNECE STANDARD FFV-42. In *concerning the marketing and commercial quality control of AVOCADOS*. New York and Geneva: United Nations.

United Nations Environment Programme. (2021). *Food Waste Index Report 2021*.

Veit, A., Wilber, M., & Belongie, S. (2016). Residual networks behave like ensembles of relatively shallow networks. *Advances in neural information processing systems*, *29*. https://doi.org/https://doi.org/10.48550/arXiv.1605.06431

Voloşencu, C. (2022). *MATLAB Applications in Engineering*. IntechOpen. https://doi.org/http://dx.doi.org/10.5772/intechopen.91588

Walter, A., Finger, R., Huber, R., & Buchmann, N. (2017). Opinion: Smart farming is key to developing sustainable agriculture. *Proc Natl Acad Sci U S A*, *114*(24), 6148-6150. https://doi.org/10.1073/pnas.1707462114

Wedding, B. B., Wright, C., Grauf, S., White, R. D., Tilse, B., & Gadek, P. (2013). Effects of seasonal variability on FT-NIR prediction of dry matter content for whole 'Hass' avocado fruit. *Postharvest Biology and Technology*, *75*, 9-16. https://doi.org/10.1016/j.postharvbio.2012.04.016

Weiss, K., Khoshgoftaar, T. M., & Wang, D. (2016). A survey of transfer learning. *Journal of Big Data*, *3*(1). https://doi.org/10.1186/s40537-016-0043-6

Woolf, A. B., Arpaia, M. L., Defilippi, B. G., & Bower, J. P. (2020). Subtropical fruits: Avocados. In M. I. Gil & R. Beaudry (Eds.), *Controlled and Modified Atmospheres for Fresh and Fresh-Cut Produce*. Academic Press.

Wu, C.-T., Roan, S.-F., Hsiung, T.-C., Chen, I.-Z., Shyr, J.-J., & Wakana, A. (2011). Effect of harvest maturity and heat pretreatment on the quality of low temperature storage avocados in Taiwan. *Journal of the Faculty of Agriculture, Kyushu University*, *56*(2), 255-262. https://doi.org/10.5109/20318

Appendices

I. Scripts

I.I. Training Scripts

```
n = 5; %defining the number of classifications [1-5]
 imT = imageDatastore(['1_TRAINING\'],'IncludeSubfolders',↙
true,'LabelSource','foldernames'); %sourcing labels from folder names
 imT.ReadFcn = @(loc)imresize(imread(loc),[227,227]); %converting images to alexnet↙
size

 fc = fullyConnectedLayer(n); %a fully connected layer multiplies the input by a↙
weight matrix and then adds a bias vector
 five_net = alexnet; %loading pretrained network
 ly = five_net.Layers;
 ly(23) = fc; %matching fully connected layer to the weight matrix and bias vector
 cl = classificationLayer;
 ly(25) = cl; %defining output layer as the classification layer
 learning_rate = 0.0001; %fixed learning rate - smaller takes longer but achieves↙
better results
 opts = trainingOptions("rmsprop","InitialLearnRate",learning_rate,'MaxEpochs',↙
30,'MiniBatchSize',64,'Plots','training-progress'); %defining training options based↙
on the relevant parameters
 [five_net,info] = trainNetwork(imT, ly, opts); %running the training network
 save five_net
```

Figure i - Training script for the non-discriminative 5-stage index CNN based on a pretrained AlexNet.

I.II. Testing and Validation Scripts

```
load('five_net.mat'); %load the previously trained network

%% test
imTest = imageDatastore(['2_TESTING\'],'IncludeSubfolders',↙
true,'LabelSource','foldernames'); %sourcing labels from folder names
imTest .ReadFcn = @(loc)imresize(imread(loc),[227,227]); %converting images to alexnet↙
size
%load nine_net; %load the previously trained network
[predict,scores] = classify(five_net,imTest);
predictnum = cellstr(predict);
a=[];
for i = 1:length(predictnum)
   a(i) = sscanf(predictnum{i},'s%d');
end
names = cellstr(imTest.Labels);
b=[];
for i = 1:length(names)
   b(i) = sscanf(names{i},'s%d');
end

m = 0; %defining margin of error

pred=[];
for i=1:length(a)

    if a(i)==1

        pred(i) =  (a(i)==b(i) |a(i)==b(i)+m);

    elseif a(i)==2

        pred(i) =  (a(i)==b(i)-m | a(i)==b(i) |a(i)==b(i)+m);


    elseif a(i)==3

        pred(i) =  (a(i)==b(i)-m | a(i)==b(i) |a(i)==b(i)+m);


    elseif a(i)==4

        pred(i) =  (a(i)==b(i)-m | a(i)==b(i) |a(i)==b(i)+m);

    elseif a(i)==5

        pred(i) = (a(i)==b(i)-m | a(i)==b(i));

       end
end


s = size(pred);
acc = sum(pred)/s(2);
fprintf('The accuracy of the test set is %f %% \n',acc*100);
```

Figure ii - Testing and validation script - part 1

```
%% validation
imVAL = imageDatastore(['3_VALIDATION\'],'IncludeSubfolders',↙
true,'LabelSource','foldernames'); %sourcing labels from folder names
imVAL .ReadFcn = @(loc)imresize(imread(loc),[227,227]); %converting images to alexnet↙
size
[predict,scores] = classify(five_net,imVAL);
predictnum = cellstr(predict);
a=[];
for i = 1:length(predictnum)
   a(i) = sscanf(predictnum{i},'s%d');
end
names = cellstr(imVAL.Labels);

b=[];
for i = 1:length(names)
   b(i) = sscanf(names{i},'s%d');
end

pred=[];
for i=1:length(a)

    if a(i)==1

        pred(i) =  (a(i)==b(i) |a(i)==b(i)+m);

    elseif a(i)==2

        pred(i) =  (a(i)==b(i)-m | a(i)==b(i) |a(i)==b(i)+m);


    elseif a(i)==3

        pred(i) =  (a(i)==b(i)-m | a(i)==b(i) |a(i)==b(i)+m);


    elseif a(i)==4

        pred(i) =  (a(i)==b(i)-m | a(i)==b(i) |a(i)==b(i)+m);

    elseif a(i)==5

        pred(i) = (a(i)==b(i)-m | a(i)==b(i));

       end
end


s = size(pred);
acc = sum(pred)/s(2);
fprintf('The accuracy of the val set is %f %% \n',acc*100);
```

Figure iii - Testing and validation script - part 2

II. Designed Networks Analysis

II.I. Analysis of the AlexNet-based Models

Table i - Layer architecture analysis for the AlexNet-based networks (5 outputs).

ANALYSIS RESULT

	Name	Type	Activa...	Learnables
1	data 227×227×3 images with 'zerocenter' normalization	Image Input	227×227×3	-
2	conv1 96 11×11×3 convolutions with stride [4 4] and padding [0 0 0 0]	Convolution	55×55×96	Weights 11×11×3×96 Bias 1×1×96
3	relu1 ReLU	ReLU	55×55×96	-
4	norm1 cross channel normalization with 5 channels per element	Cross Channel Normalization	55×55×96	-
5	pool1 3×3 max pooling with stride [2 2] and padding [0 0 0 0]	Max Pooling	27×27×96	-
6	conv2 2 groups of 128 5×5×48 convolutions with stride [1 1] and padding [2 2 2 2]	Grouped Convolution	27×27×256	Weights 5×5×48×128×2 Bias 1×1×128×2
7	relu2 ReLU	ReLU	27×27×256	-
8	norm2 cross channel normalization with 5 channels per element	Cross Channel Normalization	27×27×256	-
9	pool2 3×3 max pooling with stride [2 2] and padding [0 0 0 0]	Max Pooling	13×13×256	-
10	conv3 384 3×3×256 convolutions with stride [1 1] and padding [1 1 1 1]	Convolution	13×13×384	Weights 3×3×256×384 Bias 1×1×384
11	relu3 ReLU	ReLU	13×13×384	-
12	conv4 2 groups of 192 3×3×192 convolutions with stride [1 1] and padding [1 1 1 1]	Grouped Convolution	13×13×384	Weights 3×3×192×192×2 Bias 1×1×192×2
13	relu4 ReLU	ReLU	13×13×384	-
14	conv5 2 groups of 128 3×3×192 convolutions with stride [1 1] and padding [1 1 1 1]	Grouped Convolution	13×13×256	Weights 3×3×192×128×2 Bias 1×1×128×2
15	relu5 ReLU	ReLU	13×13×256	-
16	pool5 3×3 max pooling with stride [2 2] and padding [0 0 0 0]	Max Pooling	6×6×256	-
17	fc6 4096 fully connected layer	Fully Connected	1×1×4096	Weights 4096×9216 Bias 4096×1
18	relu6 ReLU	ReLU	1×1×4096	-
19	drop6 50% dropout	Dropout	1×1×4096	-
20	fc7 4096 fully connected layer	Fully Connected	1×1×4096	Weights 4096×4096 Bias 4096×1
21	relu7 ReLU	ReLU	1×1×4096	-
22	drop7 50% dropout	Dropout	1×1×4096	-
23	fc 5 fully connected layer	Fully Connected	1×1×5	Weights 5×4096 Bias 5×1
24	prob softmax	Softmax	1×1×5	-
25	classoutput crossentropyex	Classification Output	1×1×5	-

II.II. Analysis of the ResNet-18-based Models

Table ii - Layer architecture analysis for the ResNet-18-based networks (5 outputs). (1/3)

ANALYSIS RESULT

	Name	Type	Activations	Learnables
1	data 224×224×3 images with 'zscore' normalization	Image Input	224×224×3	-
2	conv1 64 7×7×3 convolutions with stride [2 2] and padding [3 3 3 3]	Convolution	112×112×64	Weights 7×7×3×64 Bias 1×1×64
3	bn_conv1 Batch normalization with 64 channels	Batch Normalization	112×112×64	Offset 1×1×64 Scale 1×1×64
4	conv1_relu ReLU	ReLU	112×112×64	-
5	pool1 3×3 max pooling with stride [2 2] and padding [1 1 1 1]	Max Pooling	56×56×64	-
6	res2a_branch2a 64 3×3×64 convolutions with stride [1 1] and padding [1 1 1 1]	Convolution	56×56×64	Weights 3×3×64×64 Bias 1×1×64
7	bn2a_branch2a Batch normalization with 64 channels	Batch Normalization	56×56×64	Offset 1×1×64 Scale 1×1×64
8	res2a_branch2a_relu ReLU	ReLU	56×56×64	-
9	res2a_branch2b 64 3×3×64 convolutions with stride [1 1] and padding [1 1 1 1]	Convolution	56×56×64	Weights 3×3×64×64 Bias 1×1×64
10	bn2a_branch2b Batch normalization with 64 channels	Batch Normalization	56×56×64	Offset 1×1×64 Scale 1×1×64
11	res2a Element-wise addition of 2 inputs	Addition	56×56×64	-
12	res2a_relu ReLU	ReLU	56×56×64	-
13	res2b_branch2a 64 3×3×64 convolutions with stride [1 1] and padding [1 1 1 1]	Convolution	56×56×64	Weights 3×3×64×64 Bias 1×1×64
14	bn2b_branch2a Batch normalization with 64 channels	Batch Normalization	56×56×64	Offset 1×1×64 Scale 1×1×64
15	res2b_branch2a_relu ReLU	ReLU	56×56×64	-
16	res2b_branch2b 64 3×3×64 convolutions with stride [1 1] and padding [1 1 1 1]	Convolution	56×56×64	Weights 3×3×64×64 Bias 1×1×64
17	bn2b_branch2b Batch normalization with 64 channels	Batch Normalization	56×56×64	Offset 1×1×64 Scale 1×1×64
18	res2b Element-wise addition of 2 inputs	Addition	56×56×64	-
19	res2b_relu ReLU	ReLU	56×56×64	-
20	res3a_branch2a 128 3×3×64 convolutions with stride [2 2] and padding [1 1 1 1]	Convolution	28×28×128	Weights 3×3×64×128 Bias 1×1×128
21	bn3a_branch2a Batch normalization with 128 channels	Batch Normalization	28×28×128	Offset 1×1×128 Scale 1×1×128
22	res3a_branch2a_relu ReLU	ReLU	28×28×128	-
23	res3a_branch2b 128 3×3×128 convolutions with stride [1 1] and padding [1 1 1 1]	Convolution	28×28×128	Weights 3×3×128×128 Bias 1×1×128
24	bn3a_branch2b Batch normalization with 128 channels	Batch Normalization	28×28×128	Offset 1×1×128 Scale 1×1×128
25	res3a_branch1 128 1×1×64 convolutions with stride [2 2] and padding [0 0 0 0]	Convolution	28×28×128	Weights 1×1×64×128 Bias 1×1×128

Table ii - Layer architecture analysis for the ResNet-18-based networks (5 outputs). (2/3)

26	bn3a_branch1 Batch normalization with 128 channels	Batch Normalization	28×28×128	Offset 1×1×128 Scale 1×1×128
27	res3a Element-wise addition of 2 inputs	Addition	28×28×128	-
28	res3a_relu ReLU	ReLU	28×28×128	-
29	res3b_branch2a 128 3×3×128 convolutions with stride [1 1] and padding [1 1 1 1]	Convolution	28×28×128	Weights 3×3×128×128 Bias 1×1×128
30	bn3b_branch2a Batch normalization with 128 channels	Batch Normalization	28×28×128	Offset 1×1×128 Scale 1×1×128
31	res3b_branch2a_relu ReLU	ReLU	28×28×128	-
32	res3b_branch2b 128 3×3×128 convolutions with stride [1 1] and padding [1 1 1 1]	Convolution	28×28×128	Weights 3×3×128×128 Bias 1×1×128
33	bn3b_branch2b Batch normalization with 128 channels	Batch Normalization	28×28×128	Offset 1×1×128 Scale 1×1×128
34	res3b Element-wise addition of 2 inputs	Addition	28×28×128	-
35	res3b_relu ReLU	ReLU	28×28×128	-
36	res4a_branch2a 256 3×3×128 convolutions with stride [2 2] and padding [1 1 1 1]	Convolution	14×14×256	Weights 3×3×128×256 Bias 1×1×256
37	bn4a_branch2a Batch normalization with 256 channels	Batch Normalization	14×14×256	Offset 1×1×256 Scale 1×1×256
38	res4a_branch2a_relu ReLU	ReLU	14×14×256	-
39	res4a_branch2b 256 3×3×256 convolutions with stride [1 1] and padding [1 1 1 1]	Convolution	14×14×256	Weights 3×3×256×256 Bias 1×1×256
40	bn4a_branch2b Batch normalization with 256 channels	Batch Normalization	14×14×256	Offset 1×1×256 Scale 1×1×256
41	res4a_branch1 256 1×1×128 convolutions with stride [2 2] and padding [0 0 0 0]	Convolution	14×14×256	Weights 1×1×128×256 Bias 1×1×256
42	bn4a_branch1 Batch normalization with 256 channels	Batch Normalization	14×14×256	Offset 1×1×256 Scale 1×1×256
43	res4a Element-wise addition of 2 inputs	Addition	14×14×256	-
44	res4a_relu ReLU	ReLU	14×14×256	-
45	res4b_branch2a 256 3×3×256 convolutions with stride [1 1] and padding [1 1 1 1]	Convolution	14×14×256	Weights 3×3×256×256 Bias 1×1×256
46	bn4b_branch2a Batch normalization with 256 channels	Batch Normalization	14×14×256	Offset 1×1×256 Scale 1×1×256
47	res4b_branch2a_relu ReLU	ReLU	14×14×256	-
48	res4b_branch2b 256 3×3×256 convolutions with stride [1 1] and padding [1 1 1 1]	Convolution	14×14×256	Weights 3×3×256×256 Bias 1×1×256
49	bn4b_branch2b Batch normalization with 256 channels	Batch Normalization	14×14×256	Offset 1×1×256 Scale 1×1×256
50	res4b Element-wise addition of 2 inputs	Addition	14×14×256	-

Table ii - Layer architecture analysis for the ResNet-18-based networks (5 outputs). (3/3)

51	res4b_relu ReLU	ReLU	14×14×256	-
52	res5a_branch2a 512 3×3×256 convolutions with stride [2 2] and padding [1 1 1 1]	Convolution	7×7×512	Weights 3×3×256×512 Bias 1×1×512
53	bn5a_branch2a Batch normalization with 512 channels	Batch Normalization	7×7×512	Offset 1×1×512 Scale 1×1×512
54	res5a_branch2a_relu ReLU	ReLU	7×7×512	-
55	res5a_branch2b 512 3×3×512 convolutions with stride [1 1] and padding [1 1 1 1]	Convolution	7×7×512	Weights 3×3×512×512 Bias 1×1×512
56	res5a_branch1 512 1×1×256 convolutions with stride [2 2] and padding [0 0 0 0]	Convolution	7×7×512	Weights 1×1×256×512 Bias 1×1×512
57	bn5a_branch1 Batch normalization with 512 channels	Batch Normalization	7×7×512	Offset 1×1×512 Scale 1×1×512
58	bn5a_branch2b Batch normalization with 512 channels	Batch Normalization	7×7×512	Offset 1×1×512 Scale 1×1×512
59	res5a Element-wise addition of 2 inputs	Addition	7×7×512	-
60	res5a_relu ReLU	ReLU	7×7×512	-
61	res5b_branch2a 512 3×3×512 convolutions with stride [1 1] and padding [1 1 1 1]	Convolution	7×7×512	Weights 3×3×512×512 Bias 1×1×512
62	bn5b_branch2a Batch normalization with 512 channels	Batch Normalization	7×7×512	Offset 1×1×512 Scale 1×1×512
63	res5b_branch2a_relu ReLU	ReLU	7×7×512	-
64	res5b_branch2b 512 3×3×512 convolutions with stride [1 1] and padding [1 1 1 1]	Convolution	7×7×512	Weights 3×3×512×512 Bias 1×1×512
65	bn5b_branch2b Batch normalization with 512 channels	Batch Normalization	7×7×512	Offset 1×1×512 Scale 1×1×512
66	res5b Element-wise addition of 2 inputs	Addition	7×7×512	-
67	res5b_relu ReLU	ReLU	7×7×512	-
68	pool5 Global average pooling	Global Average Pooling	1×1×512	-
69	fc 5 fully connected layer	Fully Connected	1×1×5	Weights 5×512 Bias 5×1
70	prob softmax	Softmax	1×1×5	-
71	classoutput crossentropyex	Classification Output	1×1×5	-

III. Example of Training Progress

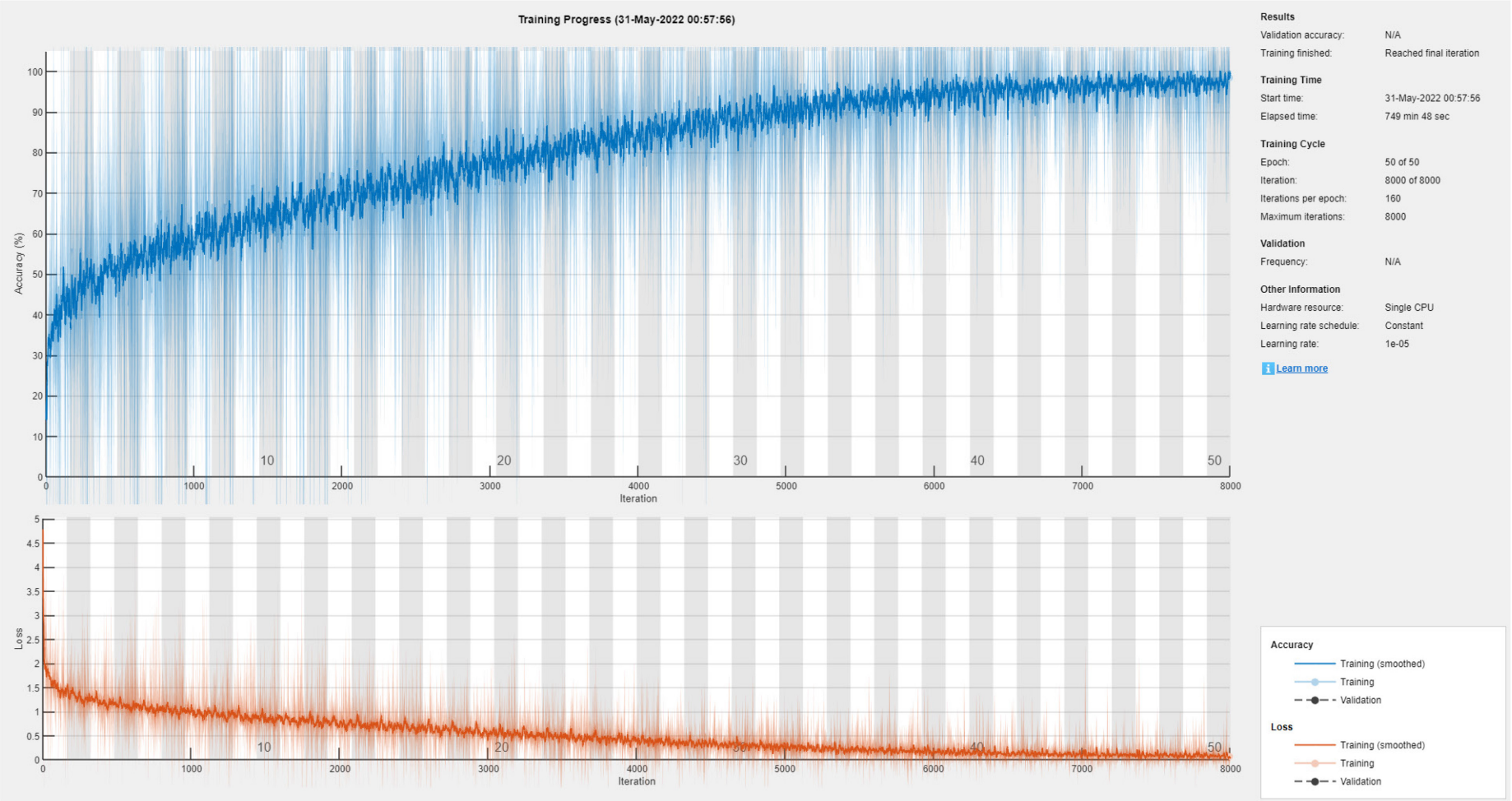

Figure iv - Training iterations for the non-discriminative 9-stage index ResNet 18 network.